

RESEARCH ARTICLE

Dynamic Pattern of HOXB9 Protein Localization during Oocyte Maturation and Early Embryonic Development in Mammals

Caroline Sauvegarde¹, Delphine Paul¹, Laure Bridoux¹, Alice Jouneau², Séverine Degrelle^{3,4,5}, Isabelle Hue², René Rezsohazy¹, Isabelle Donnay^{1*}

1 Biologie Moléculaire et Cellulaire Animale (AMCB), Institut des Sciences de la Vie (ISV), Université catholique de Louvain, Louvain-la-Neuve, Belgium, **2** UMR BDR, INRA, ENVA, Université Paris Saclay, Jouy-en-Josas, France, **3** Institut National de la Santé et de la Recherche Médicale (INSERM), UMR-S1139, U767, Faculté des Sciences Pharmaceutiques et Biologiques, Paris, France, **4** Université Paris Descartes, Sorbonne Paris Cité, Paris, France, **5** PremUp Foundation, Paris, France

* isabelle.donnay@uclouvain.be



OPEN ACCESS

Citation: Sauvegarde C, Paul D, Bridoux L, Jouneau A, Degrelle S, Hue I, et al. (2016) Dynamic Pattern of HOXB9 Protein Localization during Oocyte Maturation and Early Embryonic Development in Mammals. PLoS ONE 11(10): e0165898. doi:10.1371/journal.pone.0165898

Editor: Jason Glenn Knott, Michigan State University, UNITED STATES

Received: July 1, 2016

Accepted: October 1, 2016

Published: October 31, 2016

Copyright: © 2016 Sauvegarde et al. This is an open access article distributed under the terms of the [Creative Commons Attribution License](https://creativecommons.org/licenses/by/4.0/), which permits unrestricted use, distribution, and reproduction in any medium, provided the original author and source are credited.

Data Availability Statement: All relevant data are within the paper and its Supporting Information files.

Funding: This work was supported by a FRFC grant from Fonds National de la Recherche Scientifique (Belgium – Grant number : 2.4566.07) ; Action de Recherche Concertée from the Communauté française (Belgium) ; STSM grant from COST Action FA0702 (Gemini). The funders had no role in study design, data collection and analysis, decision to publish, or preparation of the manuscript.

Abstract

Background

We previously showed that the homeodomain transcription factor HOXB9 is expressed in mammalian oocytes and early embryos. However, a systematic and exhaustive study of the localization of the HOXB9 protein, and HOX proteins in general, during mammalian early embryonic development has so far never been performed.

Results

The distribution of HOXB9 proteins in oocytes and the early embryo was characterized by immunofluorescence from the immature oocyte stage to the peri-gastrulation period in both the mouse and the bovine. HOXB9 was detected at all studied stages with a dynamic expression pattern. Its distribution was well conserved between the two species until the blastocyst stage and was mainly nuclear. From that stage on, trophoblastic cells always showed a strong nuclear staining, while the inner cell mass and the derived cell lines showed important dynamic variations both in staining intensity and in intra-cellular localization. Indeed, HOXB9 appeared to be progressively downregulated in epiblast cells and only reappeared after gastrulation had well progressed. The protein was also detected in the primitive endoderm and its derivatives with a distinctive presence in apical vacuoles of mouse visceral endoderm cells.

Conclusions

Together, these results could suggest the existence of unsuspected functions for HOXB9 during early embryonic development in mammals.

Competing Interests: The authors have declared that no competing interests exist.

Introduction

HOXB9 is a homeodomain transcription factor of the HOX family which is well conserved within the animal kingdom. In mammals, there are 39 HOX genes organized into four chromosomal complexes (A, B, C and D) and defining 13 groups of paralogues numbered from 1 to 13. From the gastrulation stage onward, HOX proteins are known to be involved in the patterning of the anterior-posterior axis of the embryo, in limb development and in organ formation [1–4]. They have multiple functions in cell proliferation, specification and death (reviewed in [5, 6]). Besides their role as regulators of gene expression, they are involved in non-transcriptional functions such as DNA replication, DNA repair and mRNA translation (reviewed in [7]). HOXB9, in particular, takes part in the formation of the rib cage and contributes to forelimbs development [4, 8, 9]. Homozygous mice present abnormalities of the sternum, fusion of the anterior ribs and attachment of the eight ribs to the sternum. In the adult, it is involved in blood cell differentiation [10] and development of the mammary epithelium during gestation and lactation [11].

As for most *Hox* genes, the expression pattern of *Hoxb9* has been well-described in the mouse, from the gastrulation stage on, and paralleled to its roles in patterning the main body axis and the forelimbs. After gastrulation, mouse *Hoxb9* mRNA are detected first at the early headfold (EHF) stage, in the primitive streak and adjacent mesoderm, while no expression is detected in late allantoic bud (LB) stage [12–14]. During the course of embryogenesis, *Hoxb9* is expressed in the neural tube as well as in the paraxial mesoderm and its derivatives. The most anterior limit of expression in the neural tube is reached at embryonic day 10.5 (E10.5) at the level of somite 6 (first cervical somite—[8]). Little data regarding HOX gene expression are available for the bovine embryo around gastrulation or thereafter [15–17]. However, a transcriptomic study revealed HOXB9 expression in bovine embryos from day 7 to day 19 post-insemination (D7 to D19—[17]). Moreover, data concerning abundance and expression of HOX proteins are largely lacking for the majority of developmental stages in most mammalian species.

Although HOX proteins are best known for their roles in the context of embryo shaping in relationship with gastrulation, several HOX transcripts have been detected quite earlier during development in a number of mammalian species [18–27]. In particular, we have previously shown that HOXB9 transcripts are present in oocytes and early embryos in the mouse and bovine [24]. In the bovine, the relative expression of HOXB9 increases between the immature oocyte and the zygote stage, further increases at the 5- to 8-cell stage and peaks at the morula stage before decreasing at the blastocyst stage. In the mouse, *Hoxb9* transcripts are also detected at all those early developmental stages. Zygotic and maternal HOXB9 does not appear to be crucial for oocyte/embryo development since *Hoxb9*^{-/-} homozygous mice are obtained with the expected Mendelian frequency and mutant animals of both sexes are viable and fertile [8]. However, so far no study has precisely investigated the possible impact of HOXB9 loss of function on the first embryonic stages. Moreover, the significant changes in relative transcript levels observed during early development suggest a specific regulation of HOXB9. This may be linked to specific role(s) of the protein during mammalian oocyte maturation and early embryogenesis, such as in the control of the major embryonic genome activation (EGA—[28]) or the first cell differentiation event leading to inner cell mass (ICM) and trophectoderm (TE) formation.

In the present study, we have characterized the distribution of the protein in mouse and bovine oocytes and early embryos up to the peri-gastrulation period, for the first time. To this end, specific antibodies directed to HOXB9 were carefully selected and tested for each species. Protein presence and localization were then evaluated by whole-mount immunofluorescence

or immunohistochemistry at several developmental stages. Protein markers were simultaneously used to precisely localize HOXB9 in specific cell lineages or subcellular compartments. The two mammalian models were chosen due to their differences in kinetics of development, timing of EGA, implantation (E4.5 mouse embryo is ready to implant, while bovine embryo elongates and is free in the uterus until around D21) or extra-embryonic tissue development (yolk sac wall and amnion composition as well as allantois development—[29–32]).

Materials and Methods

Chemicals were purchased from Sigma-Aldrich (Saint-Louis, USA) unless otherwise stated.

Embryo production

***In vitro* production of bovine embryos.** Bovine embryos were produced, as previously described [24]. In brief, bovine ovaries were collected at a local slaughterhouse. Cumulus-oocyte complexes (COCs) were aspirated from 3–8 mm follicles, selected and washed three times in Hepes-buffered Tissue Culture Medium 199 (TCM-199). Groups of 80 to 100 COCs were matured for 24 h at 39°C under 5% CO₂ in air in 500 µl of enriched serum-free maturation medium [33]. Frozen bull semen was kindly provided by the Association wallonne de l'Élevage (Ciney, Belgium). After thawing, living spermatozoa were isolated on a discontinuous Percoll gradient and then co-incubated with matured COCs at a final titer of 2 x 10⁶/ml for 18 h in a modified Tyrode's albumin lactate pyruvate medium supplemented with 6 mg/ml fatty acid-free fraction V BSA and 1.7 IU/ml heparin. The temperature and gas composition were the same as described for the maturation step. After fertilization, presumptive zygotes were denuded by vortexing and transferred by groups of 25 to 30 into culture droplets covered with mineral oil (FertiCult™, Fertipro, Beernem, Belgium). Culture medium consisted of modified Synthetic Oviduct Fluid [34] supplemented with BSA (4 mg/ml) and ITS (5 µg/ml of insulin, 5 µg/ml of transferrin and 5 ng/ml of selenium—[35]). Embryos were cultured at 39°C under 5% O₂, 5% CO₂ and 90% N₂.

Oocytes were harvested before and after maturation. One-cell embryos, 2-cell embryos, 5- to 8-cell embryos, 9- to 16-cell embryos and compact morulae were collected 18 h post-insemination (hpi), 26 hpi, 48 hpi, 96 hpi and 120 hpi, respectively, while blastocysts were obtained at day 6, 7, 7.5, 8, 8.5 and 9 post-insemination (D6, D7, D7.5, D8, D8.5 and D9).

Collection of *in vivo* bovine embryos. *In vivo* D7 embryos were a gift from the Association wallonne de l'Élevage (Belgium). D7 embryos were received cryopreserved and were thawed as previously described [36] with slight modifications.

After oestrus synchronization and ovarian stimulation, heifers were inseminated (day 0) and elongating bovine embryos from D11 to D18 were harvested by non-surgical flushing of the uterus [37], while D25 embryos and allantoises were collected by uterine flushing after uterus dissection at a slaughterhouse [38]. Animal use and care were performed in accordance with the International Guiding Principles for Biomedical Research involving Animals at the INRA experimental farm (registered under N° FRTB910 in the national registry) and the protocol for this study was approved by the local Ethics Committee (Comité d'Éthique en Expérimentation Animale du Centre INRA de Jouy-en-Josas et AgroParisTech [or COMETHEA], registered as 12/084 and 12/086 in the National Ethics Committee registry).

Mouse oocyte collection and embryo culture. Investigations on mice were approved by the animal ethics committee of the Université catholique de Louvain (approval 083001) and were in accordance with the European directive 2010/63/UE. For mouse euthanasia, CO₂ was administered by progressive delivery in the cage volume in accordance with European

guidelines. All experiments were carried out on F1 hybrid mice: DBA/2N x C57BL/6J (Charles River Laboratories, Brussels, Belgium).

Female mice (8- to 9-week-old) were superovulated, as previously described [24]. Immature oocytes were harvested 47 h post-eCG whereas mature oocytes were collected 14 h post-hCG injection. Superovulated mice were mated overnight (O/N) and euthanized 21 h post-hCG to collect presumptive zygotes from the oviductal ampulla. Zygotes were then denuded from their cumulus cells and cultured, as previously described [24]. Two-cell embryos, pre-compaction morulae, compact morulae, early blastocysts and blastocysts were collected 48 h (E1.5), 72 h (E2.5), 80 h (E2.8), 92 h (E3.3) and 100 h (E3.6) post-hCG injection, respectively.

Collection of *in vivo* mouse embryos. Collection of *in vivo* mouse embryos. Post-implantation embryos were produced *in vivo* and harvested after euthanasia at E4.5 by uterus flushing, and at E5.5, E6.5, E7.5 (late allantoic bud [LB] and early headfold—late headfold [EHF—LHF] stages), E7.8 (first somites stage) and E12.5 by uterus dissection. For E6.5 and later stages, Reichert's membrane was removed from the embryo to facilitate penetration of antibodies. *Hoxb9*^{-/-} E12.5 embryos were kindly provided by D. Wellik (University of Michigan, Ann Arbor, USA—[8]).

Cell culture

HEK293T cells (ATCC CRL-3216™, Molsheim, France) were cultured at 37°C under 5% CO₂ in DMEM gluta Max™-II (Gibco, Gent, Belgium) supplemented with 10% fetal bovine serum (FBS—Gibco), 100 U/ml Penicillin (Gibco), 100 µg/ml Streptomycin (Gibco) and 1 mM Na-pyruvate (Gibco).

Hox9 plasmid construction

pUC57 plasmid containing the coding region for bovine *HOXA9* (NM_001105617.2), *B9* (XM_001251856, new update on 30th December 2014: NM_001191186.1), *C9* (XM_002687231.2, new update on 30th December 2014: XM_002687231.4) or *D9* (XM_002685288.1, new update on 30th December 2014: XM_002685288.3) were purchased from GenScript (Piscataway, USA). The mouse *Hox9* expression vectors were kindly provided by D. Wellik (University of Michigan, Ann Arbor, USA). Using the Gateway[®] system, sequences of interest were transferred into a v1899 destination vector for the expression of proteins fused to a N-terminal triple-FLAG tag [39]. pCAT[®]3-vector (Genbank: U57025) was obtained from Promega (Madison, USA).

Immunostaining and imaging

Primary and secondary used antibodies are listed in Tables 1 and 2, respectively. A polyclonal anti-human HOXB9 antibody (n°1) directed against a sequence showing 100% identity with the bovine protein was selected to highlight bovine HOXB9 protein, while a polyclonal anti-human HOXB9 antibody (n°2) directed against a sequence showing 98% identity with the mouse protein was selected to detect HOXB9 in the mouse. Throughout the figures, HOXB9 staining appears in red, whatever the used fluorochromes, in order to facilitate the reading of the paper.

For each immunostaining performed in this study, a negative control without primary antibodies was involved.

Whole-mount immunofluorescence. Bovine and mouse whole-mount immunofluorescence was performed on oocytes/embryos until the blastocyst stage (bovine: until D11, mouse: until E3.5), as previously described with slight modifications [46]. In brief, oocytes/embryos were fixed in 2% paraformaldehyde (PFA) in phosphate buffered saline (PBS). A working solution of 0.5% (WS 0.5) or 0.1% (WS 0.1) PBS-Tween20 was used for the bovine and mouse,

Table 1. Primary antibodies used for proteins detection.

Antibodies	Species	Clonality	Reference	Application
BioGenex				
CDX2 ¹	Mouse	Monoclonal	#MU392A-UC ^a	IH, IF: 1/100
CDX2 ²	Mouse	Monoclonal	#AM392-5M ^b	IF: N/A
Santa Cruz Biotechnology				
DLX3 ^{3, 4}	Goat	Polyclonal	#Sc-18143	IF: 1/100
GATA4 (C-20) ^{5,6}	Goat	Polyclonal	#Sc-1237	IF: 1/50
HOXB9 (H-80, N ²)	Rabbit	Polyclonal	#Sc-66924	<ul style="list-style-type: none"> • IC, IH, IF: 1/100 • WB: 1/200
OCT3/4 (N-19) ⁵	Goat	Polyclonal	#Sc-8628	IF: 1/50
Vimentin (V9) ⁴	Mouse	Monoclonal	#Sc-6260	IF: 1/100
Sigma-Aldrich				
β-actin HRP	Mouse	Monoclonal	#A3854	WB: 1/20.000
FLAG	Mouse	Monoclonal	#F1804	<ul style="list-style-type: none"> • IC: 1/100 • WB: 1/5000
HOXB9 (N ¹)	Rabbit	Polyclonal	#AV32639	<ul style="list-style-type: none"> • IC, IH: 1/300 • IF: 1/500 • WB: 1/1000
R&D Systems				
Brachyury ⁷	Goat	Polyclonal	#AF2085	IF: 1/100
CER-1 ⁷	Rat	Monoclonal	#MAB1986	IF: 1/150
GATA6	Goat	Polyclonal	#AF1700	IF: 1/200

IF: whole-mount immunofluorescence, IH: immunohistochemistry, IC: immunocytochemistry, WB: western-blot. Antibody used for post-implantation ^a or pre-implantation ^b embryos.

¹ Blij et al. [40];

² Goossens et al. [41];

³ Degrelle et al. [42];

⁴ Hue et al. [16];

⁵ Papanayotou et al. [43];

⁶ Plusa et al. [44];

⁷ Hoshino et al. [45].

doi:10.1371/journal.pone.0165898.t001

respectively. Samples were permeabilized with 0.5% Triton X-100 in WS. They were then blocked in 10% BSA in WS, followed by incubation in primary solution (1% BSA in WS). After incubation with the primary antibody, samples were washed in WS and incubated with secondary antibody before being rinsed again. Embryos were mounted in Vectashield[®] containing DAPI (Vector Laboratories, Burlingame, USA) on Lab-Tek[®] chamber slides (#155411, Thermo Fisher Scientific, St Leon-Rot, Germany).

Mouse post-implantation (from E4.5 to E7.5) embryos were fixed in 4% PFA in PBS and were permeabilized with 1% Triton X-100 in 0.5% Tween20 in PBS. After blocking in 10% BSA in 0.1% Triton X-100 in PBS, they were incubated with the primary antibody diluted in PBS containing 1% BSA and 0.1% Triton X-100. Embryos were rinsed and incubated in secondary antibody solution. Finally, they were washed. All the rinsing and incubation steps were performed on an agitator plate. Embryos were mounted in Vectashield[®] containing DAPI in a circle of nail-polish drew on a slide to avoid crushing the embryo.

Temperature and incubation time of the whole-mount immunofluorescence steps are summarized in Table 3 according to the biological samples.

Table 2. Secondary antibodies used for proteins detection.

Antibodies	Species	Reference	Application
Cell Signaling			
Anti-rabbit Alexa Fluor [®] 555	Goat	#4413	• IC, IH: 1/500 • IF: 1/500 and 1/1000
Anti-mouse Alexa Fluor [®] 488	Goat	#4408	IC, IH, IF: 1/500
Santa Cruz Biotechnology			
Anti-rabbit HRP	Bovine	#Sc-2370	WB: 1/10.000
Anti-mouse HRP	Goat	#Sc-2005	WB: 1/10.000
Thermo Fisher Scientific			
Anti-goat Alexa Fluor [®] 555	Donkey	#A-21432	IF: 1/500
Anti-goat Alexa Fluor [®] 633	Donkey	#A-21082	IF: 1/400
Anti-goat Alexa Fluor [®] 647	Donkey	#A-21447	IF: 1/200
Anti-mouse Alexa Fluor [®] 488	Donkey	#A-21202	IF: 1/400
Anti-rabbit Alexa Fluor [®] 488	Donkey	#R37118	IF: 1/500
Anti-rabbit Alexa Fluor [®] 546	Donkey	#A10040	IF: 1/200

IF: whole-mount immunofluorescence, IH: immunohistochemistry, IC: immunocytochemistry, WB: western-blot.

doi:10.1371/journal.pone.0165898.t002

Immunohistochemical and immunocytochemical analysis. Bovine elongating conceptuses (D14 and D17) and allantois were fixed from 3 h to O/N in 4% PFA in PBS and incubated successively in 15% and 18% sucrose in PBS before being embedded in Tissue-Tek[®]. Serial transversal sections of 10 µm were cut with a Leica CM 3050S cryostat (Leica Biosystems, Diegem, Belgium).

E12.5 mouse embryos were washed in PBS and fixed in 4% PFA in PBS for 1 h at 4°C. Fixed embryos were then rinsed three times for 5 min in 1% PBS-Tween20 and dehydrated as followed: 5 min in a 25% MetOH, 5 min in a 50% MetOH, 5 min in a 75% MetOH and 2 times 5 min in a 100% MetOH. An inverted MetOH gradient was used to rehydrate the embryos. After O/N incubation in 30% sucrose in PBS solution, cryopreserved embryos were embedded in Shandon[™] Cryomatrix[™] (Thermo Scientific). Frozen 18 µm sections were rehydrated in PBS for 5 min.

HEK293T cells were seeded on glass coverslips coated with poly-D-lysine (0.01 mg/ml) and transfected with 500 ng of the corresponding plasmid using the jetPrime[™] system (Polyplus

Table 3. Conditions of whole-mount immunofluorescence on bovine and mouse embryos.

	Oocytes/Embryos until blastocyst stage		Mouse post-implantation stages			
	Bovine	Mouse	E4.5	E5.5	E6.5	E7.5
Fixation (RT)	1 h	20 min	30 min	30 min	30 min	30 min
Permeabilization (RT)	1 h	1 h	1 h	1 h	1 h	2 h
Blocking	1 h; RT	1 h; RT	1 h; RT	1 h; RT	O/N; 4°C	O/N; 4°C
ACI incubation (4°C)	O/N	O/N	O/N	O/N	O/N	O/N
Rinsing (RT)	3 x 5 min	3 x 5 min	3 x 5 min	3 x 20 min	3 x 60 min	3 x 60 min
ACII incubation	1 h; RT	1 h; RT	1 h; RT	O/N; 4°C	O/N; 4°C	O/N; 4°C
Rinsing (RT)	3 x 5 min	3 x 5 min	3 x 5 min	3 x 20 min	3 x 60 min	3 x 60 min

ACI: primary antibody, ACII: secondary antibody, RT: room temperature, O/N: overnight.

doi:10.1371/journal.pone.0165898.t003

transfection™, Illkirch, France), following the manufacturer's instructions. Cells were then fixed for 20 min in 4% PFA in PBS.

For immunochemistry, sections or cells were permeabilized with 0.5% Triton X-100 in WS 0.1 for 10 min at RT and blocked in 10% skimmed powder milk in WS 0.1 for 1 h at RT. Samples were then successively incubated in primary (O/N at 4°C) and secondary (1 h at RT) antibody solutions (1% BSA in WS 0.1). Antibody incubations were followed by three rinsing steps of 5 min in WS 0.1. Samples were mounted in Vectashield® containing DAPI.

Combined whole-mount immunofluorescence and immunohistochemical analysis.

D15 and D18 bovine embryos were successively submitted to a whole-mount immunofluorescence and to an immunohistochemical analysis on slices obtained after cutting the stained embryos. Briefly, embryos were fixed, dehydrated and stored at -20°C until used, as previously described [16]. Embryos were then rehydrated using a decreasing methanol gradient: 75%, 50%, and 25% for 15 min each and for 1 h in PBS. After being permeabilized in 0.5% triton in WS 0.1 for 40 min at RT, embryos were blocked with a 5% BSA IgGs free solution in WS 0.1 for 1 h at RT. Then, embryos were incubated O/N at 4°C in the primary antibody solution containing 5% BSA in WS 0.1. After rinsing, embryos were incubated with the secondary antibody solution for 1 h at RT and rinsed again before being incubated in a DAPI solution (1/20,000) for 10 min at RT. Embryos were rinsed and mounted in Fluoromount-G®. After images acquisition, the embryos were recovered and rinsed (for 2 h at RT in WS 0.1) and re-fixed in 4% PFA in PBS for 10 min at RT. Embryos were then embedded in Tissue-Tek® and 5 µm sections were obtained. Slices were dried for 15 min at RT, incubated for 10 min in PBS and permeabilized for 30 min at RT in the same permeabilization solution used for the whole-mount immunofluorescence. Embryos were then blocked and successively incubated in the primary and secondary antibody solutions, as described previously. Slices were mounted with Dako fluorescent mounting medium (Dako, Les Ulis, France).

Imaging. The labeled oocytes, embryos and cells were observed under a confocal microscope using the ZEN acquisition software (LSM710, Zeiss, Jena, Germany) or with an Axioskop 2 microscope. Images of D15 and D18 bovine embryos were acquired using a Nikon AZ100 multizoom microscope (Nikon, Amsterdam, The Netherlands) for the whole-mount or using a Lamina multilabel slide scanner (Perkin Elmer, Massachusetts, USA) for sections.

Blastocyst fluorescence signal was quantified using Nis-element 3.1 (Nikon) software. For each ICM or TE cell, the mean fluorescence intensity (i.e. mean intensity of pixels) of the nucleus was quantified and reported to the geometric mean of mean intensity of all the ICM nuclei taken as reference.

Western-blot

HEK293T cells seeded in 6-well plates were transfected with 1 µg of expression vector using the jetPrime® reagent following the instructions of the manufacturer. Proteins were extracted with IPLS buffer (20 mM Tris HCl pH 7.5, 120 mM NaCl, 0.5 mM EDTA, 0.5% Nonidet P40, protease inhibitor [#11873580001, Roche, Mannheim, Germany], 10% glycerol). After 5 min boiling, protein extracts were run on 10% SDS-PAGE gels and blotted on nitrocellulose membranes (#10600002, Amersham Biosciences, Diegem, Belgium). Membranes were blocked for 1 h at RT in 10% skimmed powder milk and were then successively incubated at 4°C with primary (O/N) and secondary (1 h) antibody solutions. Primary and HRP-conjugated secondary antibodies used are listed in Tables 1 and 2. Peroxidase activity was detected using the western lightning® Plus-ECL system (#NEL104001EA, PerkinElmer, Massachusetts, USA). Membranes were recycled by stripping (5 min in water, three times for 5 min in 0.2 M NaOH and 5 min in water) and blocked again for protein load detection using β-actin HRP (1 h at 4°C).

Statistical analysis. Statistical analyses were performed with JUMP Pro 12 software (SAS Institute, Cary, USA). The HOXB9 distribution between mouse or bovine ICM and TE cells was analyzed at each stage by comparing the ratios obtained for all nuclei with a linear mixed model. The cell lineage (ICM or TE) was considered as fixed variable, while the embryo and the experiment were considered as random variables. Interactions between embryo and experiment factors have also been analyzed using REML variance component estimates. Differences were considered significant at p-values lower than 0.05. Ratios of ICM or TE cells were compared between stages with a Welch test. For significant differences, each pair was then compared with a Student T test for unequal variances. The significant threshold was adjusted following the Bonferroni method: a p-value below $0.05/3$ (0.017) was significant.

Results

Validating antibodies for the bovine and mouse HOXB9 proteins

The specificity of the two antibodies was assayed in HEK293T cells overexpressing bovine or mouse HOXB9 protein, respectively, via two complementary approaches: western-blot detection on protein extracts (N = 3 –Fig 1A–1D) and immunofluorescence (N = 3 –Fig 1E). Moreover, to ensure that the antibodies do not recognize other HOX proteins of the paralogous group 9 (due to high sequence homology between HOX9 proteins), cells overexpressing HOXA9, HOXC9 or HOXD9 were also tested.

The western-blot performed with the anti-FLAG antibody revealed a robust expression of mouse or bovine HOX9 proteins (Fig 1A and 1C). Spots associated to the proteins were observed at molecular weights appearing slightly higher than the theoretical ones (HOXA9: ± 30 kDa, HOXB9: ± 28 kDa, HOXC9: ± 29 kDa and HOXD9: ± 35 kDa) probably due to the denaturing conditions used. Using the anti-HOXB9 antibodies, one band of high intensity was observed for both species only in cells transfected for the corresponding HOXB9 expression constructs and not for the other HOX9 paralogues (Fig 1B and 1D). This band appears at the same molecular weight as observed with the anti-FLAG antibody. This demonstrates that the selected antibodies do not cross-react with paralogous proteins thereby supporting their specificity towards HOXB9. A band corresponding to the HOXB9 protein was also detected with a lower intensity in controls (Fig 1D), confirming a basal level of expression of *HOXB9* in HEK293T cells [47]. This was further confirmed by RT-PCR. Antibody specificity was also checked by immunofluorescence for the bovine (Fig 1E) and mouse proteins. A double staining was performed with anti-HOXB9 antibody and an anti-FLAG antibody. A strong nuclear staining corresponding to FLAG-tagged HOXB9 proteins was observed with the anti-HOXB9 antibody while only the FLAG epitope was detected in FLAG-tagged HOXA9, HOXC9 or HOXD9 expressing cells.

Immunohistochemistry was also performed on E12.5 *Hoxb9*^{-/-} embryos to confirm the specificity of the antibody in the mouse (N = 2). No signal was observed in *Hoxb9*^{-/-} embryos, while in wild-type embryos HOXB9 proteins were detected in the dorsal part of the epithelium of the neural tube (Fig 1F) and with an anterior limit corresponding to the one described for *Hoxb9* transcripts [8, 48, 49].

Together, these data confirm the specificity of both HOXB9 antibodies.

HOXB9 is present in oocytes and from the zygote to the blastocyst stage in mammals

To correlate the presence of HOXB9 proteins with *HOXB9* expression profiles previously revealed in the mouse and bovine [24], distribution of proteins was characterized using whole-mount

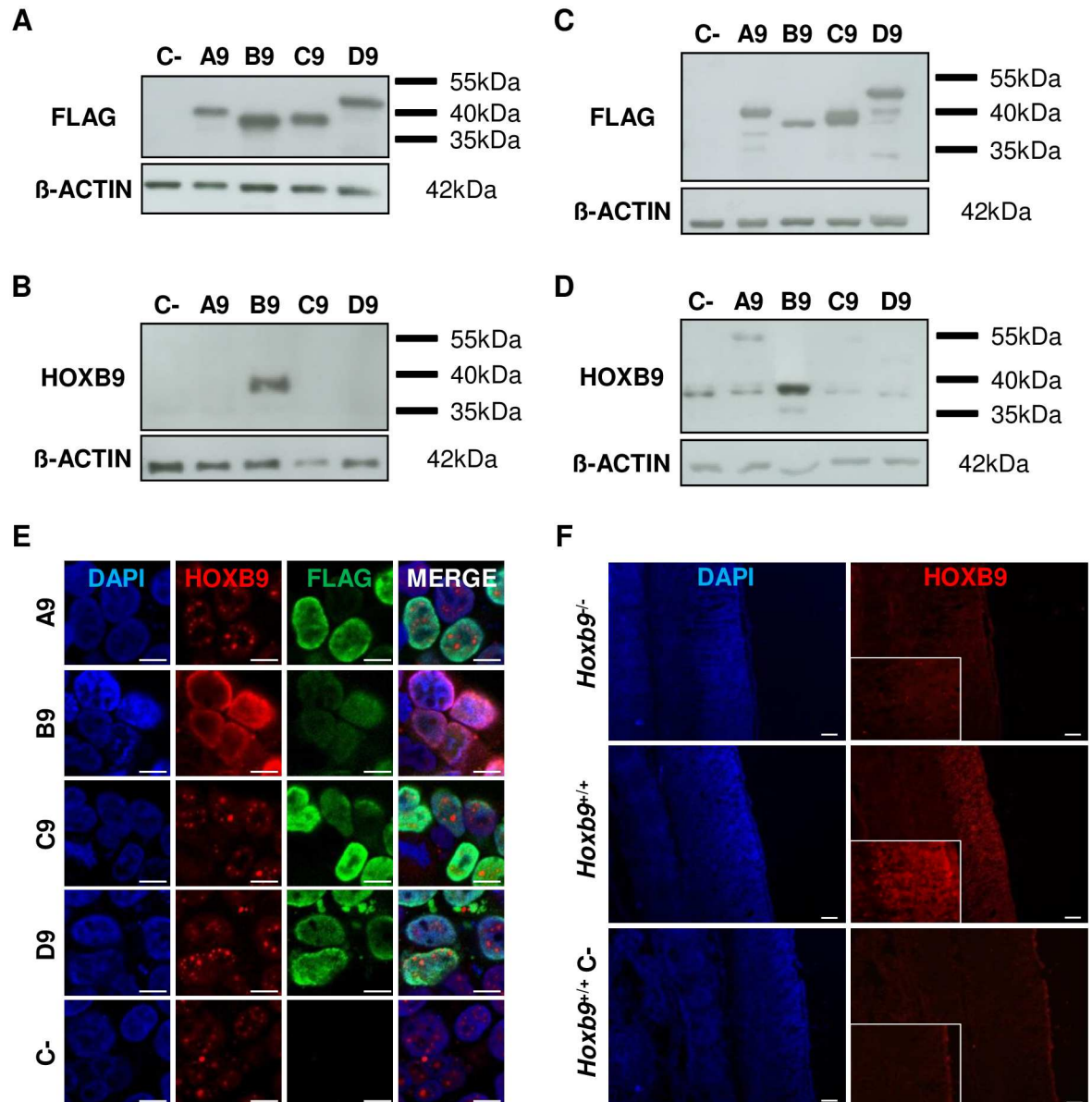


Fig 1. Analysis of specificity of the anti-HOXB9 antibodies. A-E: Overexpression of mouse (A-B) or bovine (C-E) HOXA9 (A9), HOXB9 (B9), HOXC9 (C9) or HOXD9 (D9) proteins in HEK293T cells. Each protein was fused to a FLAG tag. (A, C) Western-blot using the anti-FLAG antibody (N = 3). (B, D) Western-blot using the anti-HOXB9 antibody 1 (D) or 2 (B) (N = 3). C-: cells transfected with a control vector. The β -ACTIN was used to control protein loading. (E) HEK293T cells overexpressing the bovine HOXA9 proteins or transfected with a control vector (C-) were stained simultaneously with anti-HOXB9 (Red) and anti-FLAG (Green) antibodies and DAPI (N = 3). Representative confocal Z-section. Scale bar = 10 μ m. F: Immunofluorescence with anti-HOXB9 antibody 2 on E12.5 *Hoxb9*^{-/-} knock-out mouse embryos (N = 2). E12.5 wild-type embryos (*Hoxb9*^{+/+}) were used as positive control. *Hoxb9*^{+/+} C-: negative control without primary antibody. The boxes represent zooms on neural tube epithelium. HOXB9: Red, DAPI: Blue. Epifluorescence images. Scale bar = 100 μ m. N = number of replicates.

doi:10.1371/journal.pone.0165898.g001

immunofluorescence in oocytes and from the zygote to the blastocyst stage. For each stage, at least 3 embryos were handled at the same time and experiments were repeated at least twice.

Mouse. Mouse HOXB9 immunofluorescence was detected at all analyzed stages (Fig 2A). In mouse immature and mature oocytes, a strong HOXB9 staining overlapped with the DAPI,

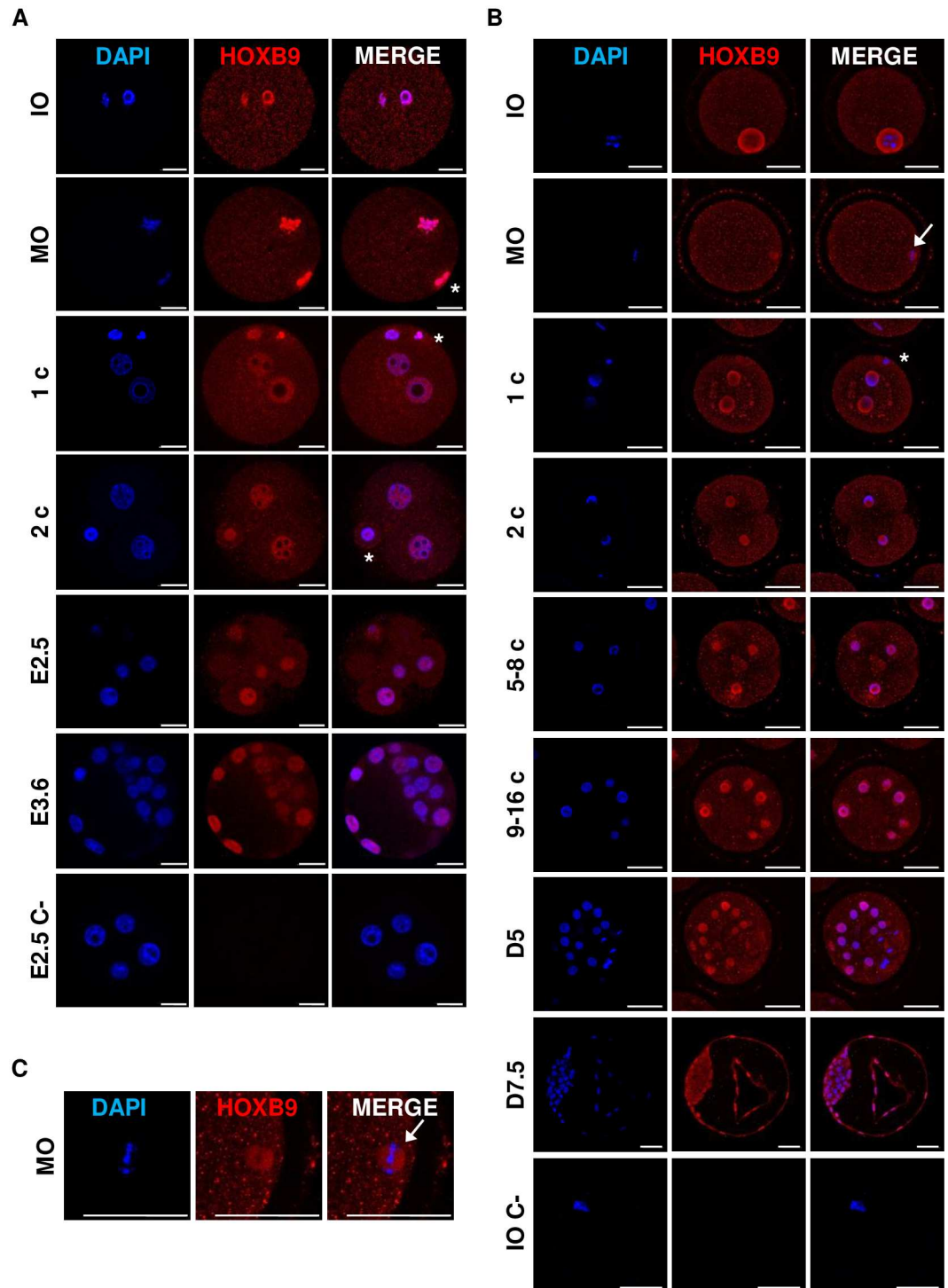


Fig 2. Mouse and bovine HOXB9 protein distribution in oocytes and from zygotes to blastocysts. A-C: Whole-mount immunofluorescence of *in vitro* cultured mouse (A) and *in vitro* produced bovine (B) embryos. Immature oocyte (IO); mature oocyte (MO); 1-cell embryo (1c); 2-cell embryo (2c); 5- to 8-cell embryo (5–8c); 9- to 16-cell embryo (9–16c); mouse pre-compaction stage (E2.5); bovine compact morula (D5); mouse blastocyst (E3.6) and bovine blastocyst (D7.5). Negative control without primary antibody are shown for E2.5 mouse embryos (E2.5 C-) and bovine IO (IO C-). (C) Zoom on bovine HOXB9 distribution at the metaphasic plate of mature oocyte. Nuclei: Blue; HOXB9: Red. The asterisk depicts polar body. White arrow shows metaphasic plate. Representative confocal Z-section. Scale bar = 20 μm (mouse) or 50 μm (bovine).

doi:10.1371/journal.pone.0165898.g002

while a fainter cytoplasmic staining was also present. A strong signal was detected in the maternal and the paternal pronuclei of zygotes as well as in polar bodies (asterisk), whereas a lighter signal was present in the cytoplasm. In 2-cell embryos and pre-compaction morulae (E2.5), HOXB9 was found in the nucleus and cytoplasm of all cells. The nuclear staining was always more prominent than the cytoplasmic one at these stages. At the blastocyst stage (E3.6), heterogeneity of HOXB9 staining was observed between ICM and TE cells, with a stronger staining in the nucleus of both polar and mural TE cells.

Bovine. As in the mouse, HOXB9 was present in bovine oocytes and throughout early embryonic development (Fig 2B). In immature oocytes, a staining was visible in the cytoplasm but the germinal vesicle was much more intensely stained. HOXB9 did not co-localize with the DAPI staining of immature and mature oocytes, conversely to the mouse. Also, in mature oocytes, HOXB9 staining was slightly more intense at the metaphasic plate for 24 out of the 28 mature oocytes analyzed (Fig 2B and 2C—arrow). From the zygote to the blastocyst stage, the presence of HOXB9 was more visible in the nuclei than in the cytoplasm, similarly to the mouse. A strong signal was detected in the maternal and the paternal pronuclei of zygotes. The polar bodies were also stained. In D7.5 blastocysts, as observed for the mouse, HOXB9 was present in both cell lineages with a stronger nuclear staining in TE cells.

These results show that mouse and bovine HOXB9 protein profiles are similar and characterized by the presence of the protein in all oocytes and embryonic cells from the zygote to the blastocyst stage, mainly in nuclei.

The HOXB9 protein is expressed differently in the two first cell lineages of mammalian blastocysts

An in-depth study of HOXB9 protein distribution in ICM and TE cells was conducted on *in vitro* cultured mouse compact morulae (E2.8) and blastocysts (E3.3 and E3.6) and on *in vitro* produced bovine embryos from early to hatched blastocysts (D6, D7.5 and D8). At least 11 mouse embryos from 2 replicates and 14 bovine embryos from 3 repetitions were analyzed at each stage. Mouse and bovine embryo development from fertilization to gastrulation is reviewed elsewhere [31, 50–57].

Mouse. All nuclei of compact morulae presented a similar staining, similarly to that previously described at the pre-compaction stage. Conversely, in E3.3 and E3.6 blastocysts, the nuclei of both polar and mural TE cells displayed increased staining compared to ICM cells nuclei (Fig 3A). A similar pattern was observed in *in vivo* produced blastocysts (Fig 3B). To confirm this observation, nuclear staining intensity was quantified and compared between ICM and TE cells. To accurately identify cells belonging to one or the other cell lineages, a co-staining with CDX2, a transcription factor specific to TE cells [58, 59], was performed (Fig 3B). Forty embryos from 3 repetitions were analyzed (total number of analyzed nuclei: ICM = 217, TE = 258). Relative fluorescence was significantly higher for TE cells than for ICM cells (linear mixed model, $p < 0.0001$ —Fig 3C) suggesting that HOXB9 is more abundant in TE than in ICM nuclei. Furthermore, a majority of E3.6 blastocysts displayed heterogeneity between ICM cells for HOXB9 nuclear staining which was not observed in E3.3 blastocysts.

Bovine. As observed for the mouse, while all cells of compacted morulae displayed a similar nuclear staining (Fig 2B), TE nuclei displayed strong staining compared to ICM at all the blastocyst stages (Fig 3D). Quantification of the staining confirmed this observation. Indeed, relative staining was significantly higher in TE cells than in ICM cells at all the blastocyst stages (linear mixed model, $p < 0.0001$ —Fig 3E). Fourteen D6 blastocysts (number of analyzed nuclei: ICM = 190 and TE = 135), 16 D7.5 blastocysts (number of analyzed nuclei: ICM = 250 and TE = 205) and 17 D8 blastocysts (number of analyzed nuclei: ICM = 264 and TE = 227)

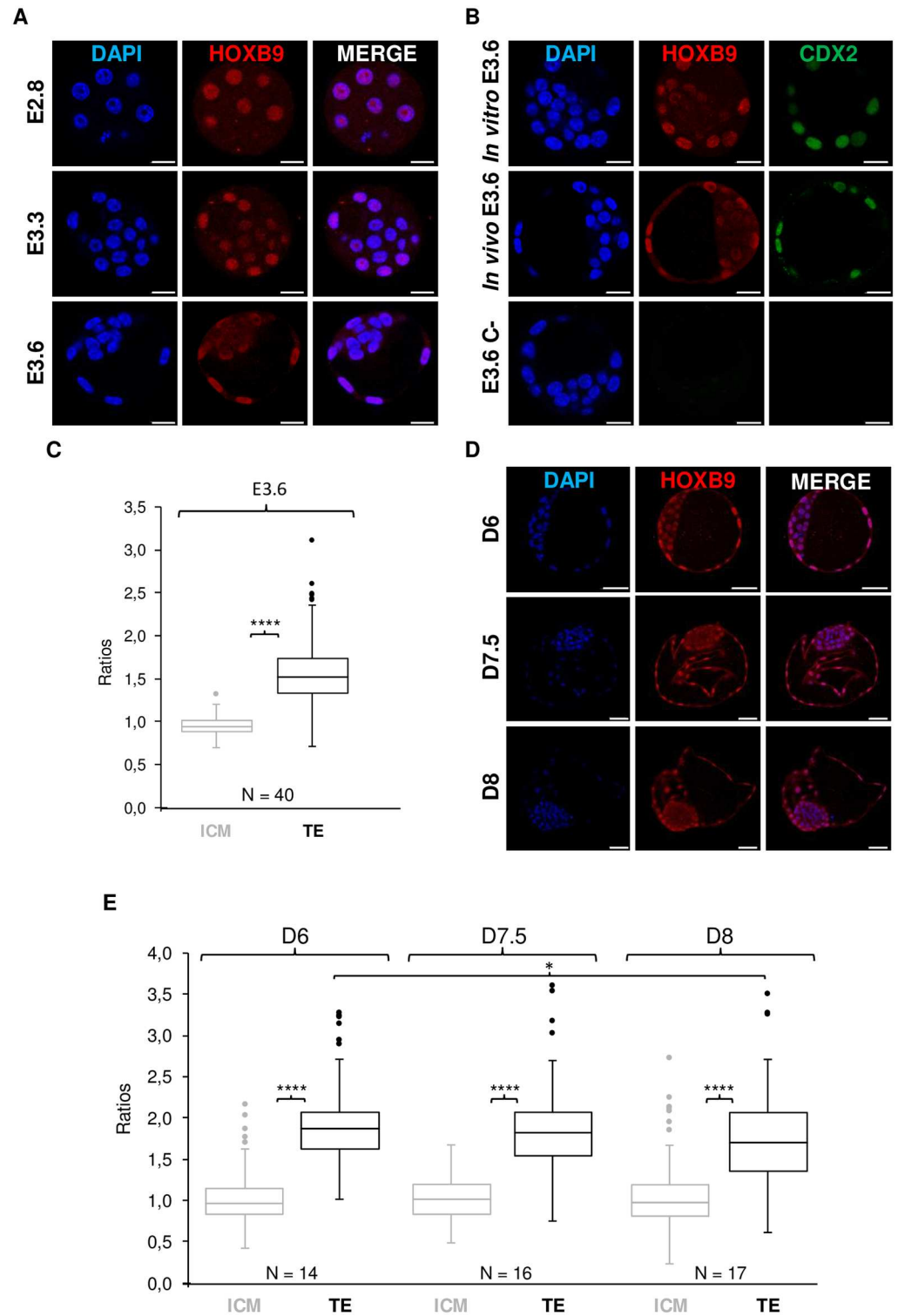


Fig 3. In-depth study of mouse and bovine HOXB9 protein distribution during the first step of cell differentiation. A-C: Mouse HOXB9 protein distribution. **D-E:** Bovine HOXB9 protein distribution. **(A-B, D)** Whole-mount immunofluorescence. Mouse compact morula at embryonic day E2.8 (E2.8); mouse blastocyst at E3.3 and E3.6 and bovine blastocyst at day 6, 7.5 and 8 post-insemination (D6, D7.5 and D8). Nuclei: Blue; HOXB9: Red; CDX2: Green. Representative confocal Z-section. Scale bar = 20 μ m (mouse) or 50 μ m (bovine). **(C, E)** Quantification of relative fluorescence corresponding to nuclear HOXB9 proteins. The boxplot

depicts the distribution of the ratios. The ends of the whiskers represent the lowest or the highest datum still within 1.5 x interquartile range. Dots correspond to outliers. N = number of analyzed embryos. * Significant difference (Linear mixed model, * = 0.01 < p < 0.05, **** = p < 0.0001).

doi:10.1371/journal.pone.0165898.g003

were analyzed. In addition, in line with observations made in E3.6 mouse blastocysts, heterogeneity of HOXB9 staining among ICM nuclei was clear from the D7.5 blastocyst stage (Fig 3D).

These results demonstrate that mouse and bovine HOXB9 nuclear proteins are equally distributed between cells in the embryo until compaction, before being reduced in ICM cells compared to TE cells. Furthermore, HOXB9 abundance in the nucleus become heterogeneous from cell to cell in ICM during blastocyst expansion.

The nuclear abundance of HOXB9 heterogeneously decreases in ICM during primitive endoderm formation

The final event in blastocyst formation is the segregation of ICM cells into the primitive endoderm (PrE) and epiblast. Precursors of these two cell lineages are present and display a salt and pepper distribution in ICM prior their final commitment (taking place at E4.5 for the mouse and at D12 for the bovine). Both of these cell types express specific markers [55, 60–62]. We hypothesized that the heterogeneity of HOXB9 staining observed between ICM cells of E3.6 mouse and D7.5–D8 bovine blastocysts could be related to the segregation of PrE and epiblast cells. To test this hypothesis, specific markers of PrE cells, namely GATA4 in the mouse [43, 44, 55, 63] and GATA6 in the bovine [61, 62], were detected by immunofluorescence. Mouse epiblast cell nuclei were also co-stained with OCT4 [43, 63, 64].

Mouse. E4.5 mouse embryos produced *in vivo* from 3 replicates (8 embryos) were analyzed. As observed in E3.6 blastocysts, all mural and polar TE cells presented a stronger nuclear HOXB9 staining than ICM cells, in which HOXB9 showed different level of expression between cells (Fig 4A). No correlation between HOXB9 and GATA4 staining could be established since GATA4 positive or negative nuclei displayed variable HOXB9 staining. Similarly, no correlation was found between OCT4 and HOXB9 staining intensities (3 replicates, 8 embryos—Fig 4A).

Bovine. *In vitro* produced blastocysts were collected from 3 replicates at D7, D8, D8.5 and D9. Moreover, *in vivo* D7 and D11 embryos were also analyzed. To verify if a similar HOXB9 pattern was observed in *in vitro* and *in vivo* embryos, HOXB9 staining was furthermore analyzed in *in vivo* produced D7 blastocysts. From D8 on, all collected blastocysts were hatched. As previously observed, TE nuclei showed stronger staining associated to HOXB9 than ICM nuclei at all analyzed stages (Fig 4B). At D7, all nuclei were positive for GATA6 and HOXB9. Moreover, half of the embryos showed heterogeneity in ICM staining for HOXB9. *In vivo* produced D7 blastocysts presented the same pattern (Fig 4C), suggesting the absence of impact of culture conditions on HOXB9 expression. In D8 hatched blastocysts, GATA6 expression displayed a “salt and pepper” pattern. All cells remained HOXB9 positive and 4 out of 6 embryos showed heterogeneity in ICM staining for HOXB9 from cell to cell nuclei. From D8.5 to D9, the majority of GATA6 positive cells were localized at the limit between ICM and the blastocoel cavity. These cells likely correspond to PrE cells. Most of them displayed a clear nuclear HOXB9 staining. In some embryos, isolated cells localized against TE were present and could also correspond to PrE cells (Fig 4B—arrows). Those cells displayed a clear HOXB9 staining. Moreover, negative GATA6 nuclei showed various intensity of HOXB9 staining. This pattern was previously observed in a small number of D8 blastocysts. At D11, PrE cells showed HOXB9 nuclear staining. It was also interesting to notice that the HOXB9 nuclear staining was

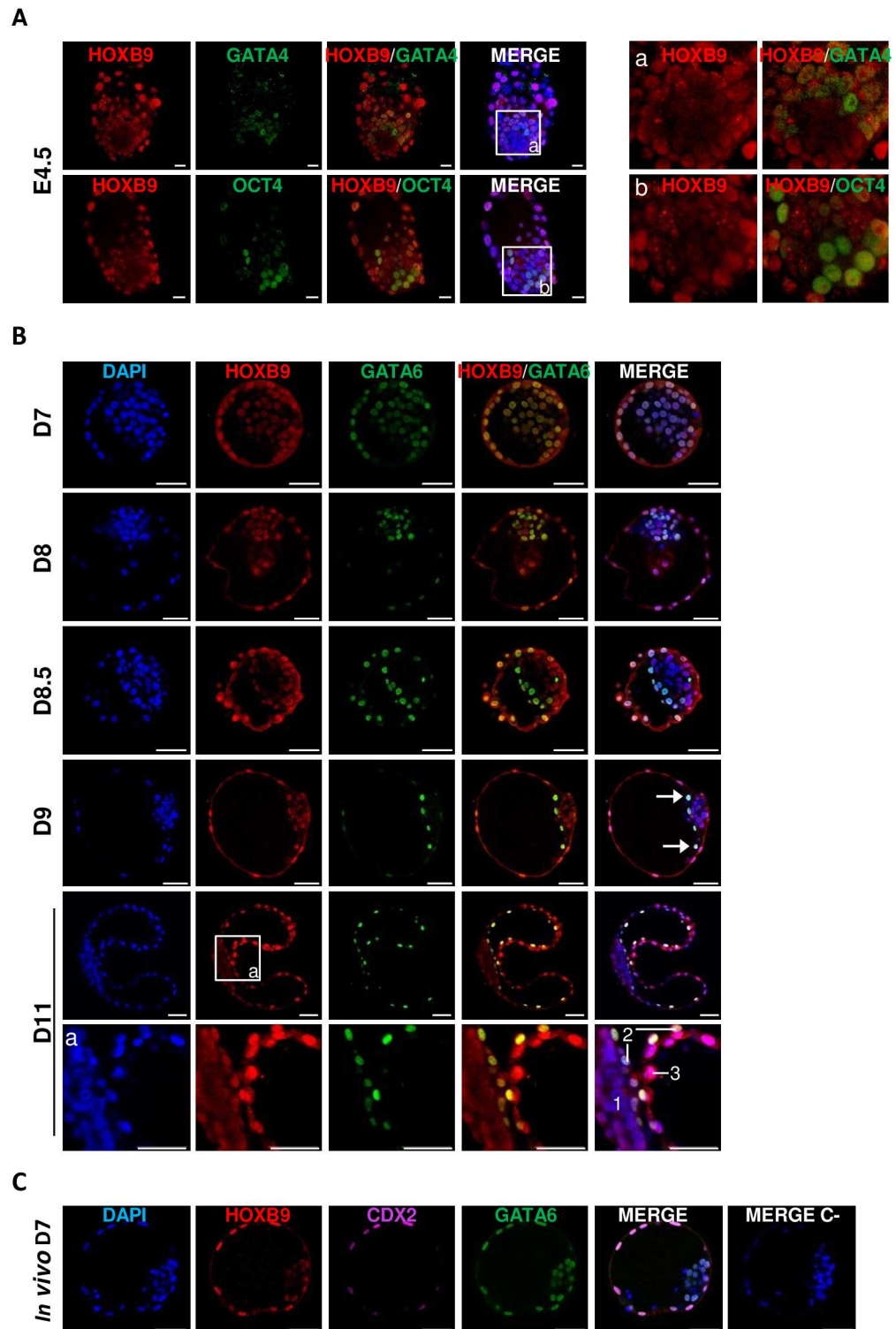


Fig 4. Mouse and bovine HOXB9 protein distribution during primitive endoderm formation. A-C: Whole-mount immunofluorescence. **(A)** Mouse *in vivo* blastocyst at E4.5. a—b: Zoom on epiblast. **(B)** Bovine *in vitro* blastocysts at day 7, 8, 8.5 and 9 post-insemination (D7; D8; D8.5 and D9) and *in vivo* embryos at day 11 post-insemination (D11). Arrows point to GATA6 positive cells that could correspond to primitive endoderm cells. Zoom on D11 bovine embryo **(a)**. 1. epiblast; 2. primitive endoderm; 3. trophoctoderm. **(C)** Bovine blastocyst produced *in vivo* at D7. Merge C-: negative control without primary

antibody. Nuclei: Blue; HOXB9: Red; GATA4/GATA6: Green; CDX2: Pink. Representative confocal Z-section. Scale bar = 20 μm (mouse) or 50 μm (bovine).

doi:10.1371/journal.pone.0165898.g004

still reduced in epiblast cells but the staining was more homogeneous between cells unlike what was observed in ICM of D7.5–9 embryos.

To conclude, neither mouse nor bovine nuclear HOXB9 proteins abundance correlates with the presence of PrE markers. However, in the bovine, once PrE formation is initiated, all corresponding cells express HOXB9 and show a strong nuclear staining of the protein, while epiblast cells display a weaker homogeneously distributed staining.

HOXB9 protein expression is restricted in mouse peri-gastrulating embryos

The localization of HOXB9 protein in the mouse was then evaluated from blastocyst implantation to post-gastrulating embryo stages, stages for which *in situ* hybridization data are available in the literature from E6.5 on [8, 12–14].

Mouse embryos produced *in vivo* were collected at E5.5, E6.5, E7.5 (LB and EHF—LHF stages, respectively) and E7.8 (first somites stage) and submitted to whole-mount immunofluorescence staining (Figs 5 and 6). At each stage, at least 3 embryos were handled in each experiment and the experiment was repeated at least twice.

At E5.5, HOXB9 displayed a strong nuclear localization in trophoblast cells located at the periphery of the ectoplacental cone (EPC), while the staining became progressively weaker and eventually disappeared in cells lying close to the center of the cone (Fig 5A1—orange arrow). Extra-embryonic ectodermal (ExE) cells were also devoid of staining (Fig 5A1). Primary trophoblastic giant cells (TGCI), derived from the mural TE cells undergoing endoreduplication [65], also presented a strong nuclear staining (Fig 5A2). Conversely, HOXB9 was barely detected in epiblast cells (Fig 5A1—section a). Embryonic (EVE) and extra-embryonic visceral endoderm (ExVE), deriving from GATA4 positive PrE cells [66, 67], showed a strong punctuated HOXB9 staining at the apical pole of cells, likely corresponding to cytoplasmic vesicles (Fig 5A—arrows—see *infra*). Nuclear staining was weaker and displayed variable intensities in these cells (Fig 5A2—arrowheads). In parietal endoderm cells, also known to express GATA4 [66, 67], HOXB9 was abundant in both the nucleus and the cytoplasm, stained cytoplasmic vesicles showing no obvious polarity in their distribution (Fig 5A2).

Visceral endoderm is well-known to be a polarized epithelium [68, 69] that supplies maternal nutrients to early mammalian embryos [70]. During normal development in the mouse (but not in ruminants), IgGs are endocytosed by VE cells [71, 72] and accumulated in vesicles called apical vacuoles (a specialized type of lysosome—[21, 73, 74]). To determine whether HOXB9 staining co-localized with these apical vacuoles, a co-staining with mouse IgGs was performed on E5.5 embryos. Fig 5A3 (arrow) depicts a clear co-localization between HOXB9 and mouse IgGs at apical vacuoles.

At the onset of gastrulation (E6.5), the superficial trophoblastic cells of EPC displayed a heterogeneous pattern for HOXB9 staining (Fig 5B5). Indeed, cells with both cytoplasmic and nuclear HOXB9 staining as well as cells with nuclear staining only were observed. Cytoplasmic HOXB9 spots, which could correspond to cytoplasmic vesicles, were also observed. The ExE remained negative for HOXB9 staining (Fig 5B1), as did epiblast cells (except some peripheral cells) that were clearly marked with OCT4 (Fig 5B1—section a). Cells from primitive streak, identified via BRACHYURY (T) expression [45, 75], were also negative for HOXB9 (Fig 5B2—section a). At this stage, EVE cells are squamous at the distal pole of the embryo, whereas they

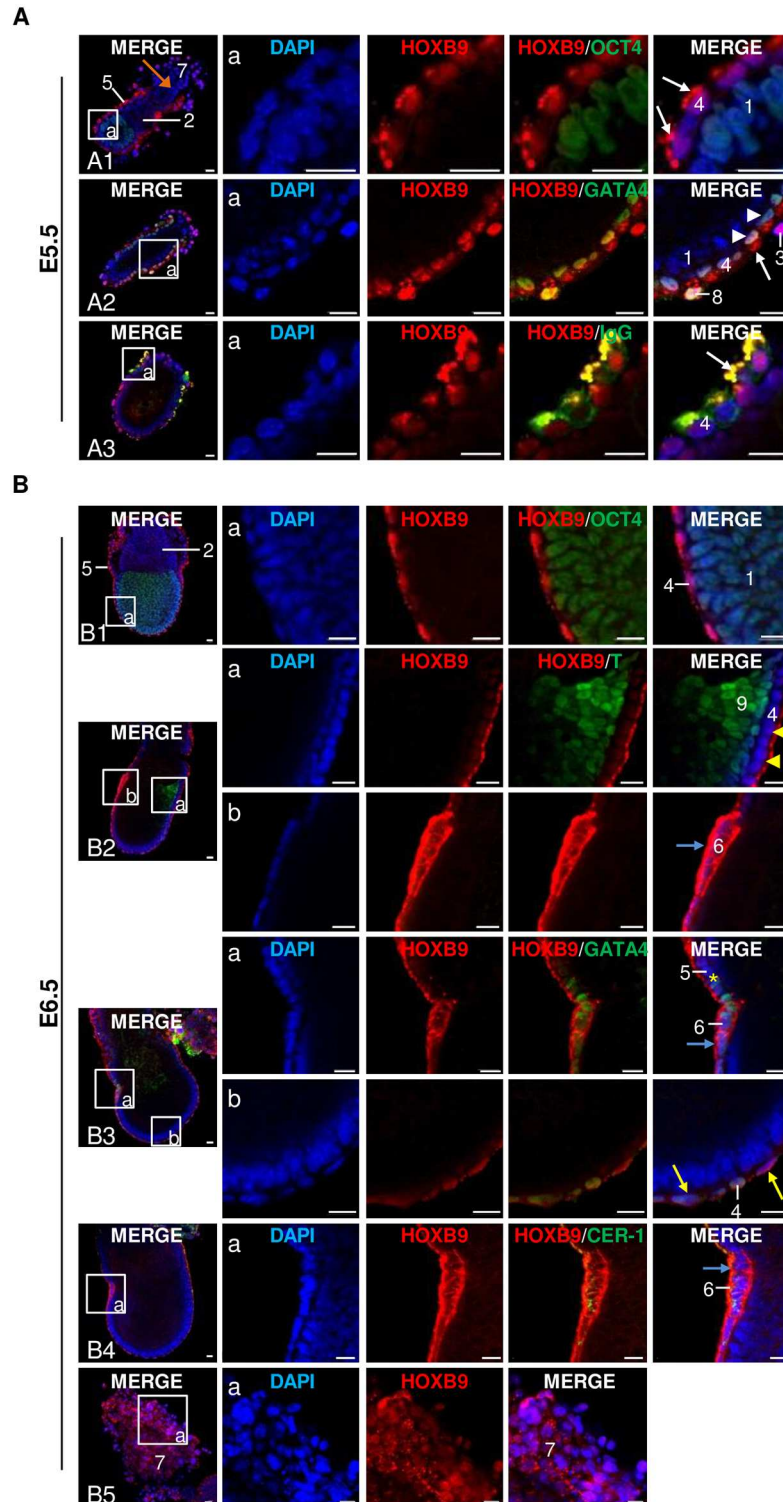


Fig 5. Mouse HOXB9 protein distribution in *in vivo* peri-gastrulating embryos: E5.5 and E6.5. A-B: Whole-mount immunofluorescence. **(A)** E5.5: HOXB9 proteins were co-stained with OCT4 **(A1)**, GATA4 **(A2)** or IgG **(A3)**. Arrows indicate HOXB9 that is localized in apical vacuoles of visceral endoderm cells. Orange arrows indicate the reduction of HOXB9 staining intensity observed in trophoblast cells in the center of the ectoplacental cone. Arrowheads indicate variation in HOXB9 nuclear staining between visceral endoderm cells. **(B)** E6.5: HOXB9 proteins were co-stained with OCT4 **(B1)**, BRACHYURY (T)—**(B2)**, GATA4

(B3) and CER-1 (B4). Zoom on the ectoplacental cone (B5). Yellow arrows, arrowheads and the asterisk show the flattened, cuboidal and columnar cells of the visceral endoderm, respectively. Blue arrows indicate the strong HOXB9 staining observed in anterior visceral endoderm cells. 1. epiblast; 2. extra-embryonic ectoderm; 3. primary trophoblastic giant cells; 4. embryonic visceral endoderm; 5. extra-embryonic visceral endoderm; 6. anterior visceral endoderm; 7. ectoplacental cone; 8. parietal endoderm; 9. primitive streak. Nuclei: Blue; HOXB9: Red; OCT4/GATA4/IgG/T/CER-1: Green. Representative confocal Z-section. Scale bar = 20 μ m.

doi:10.1371/journal.pone.0165898.g005

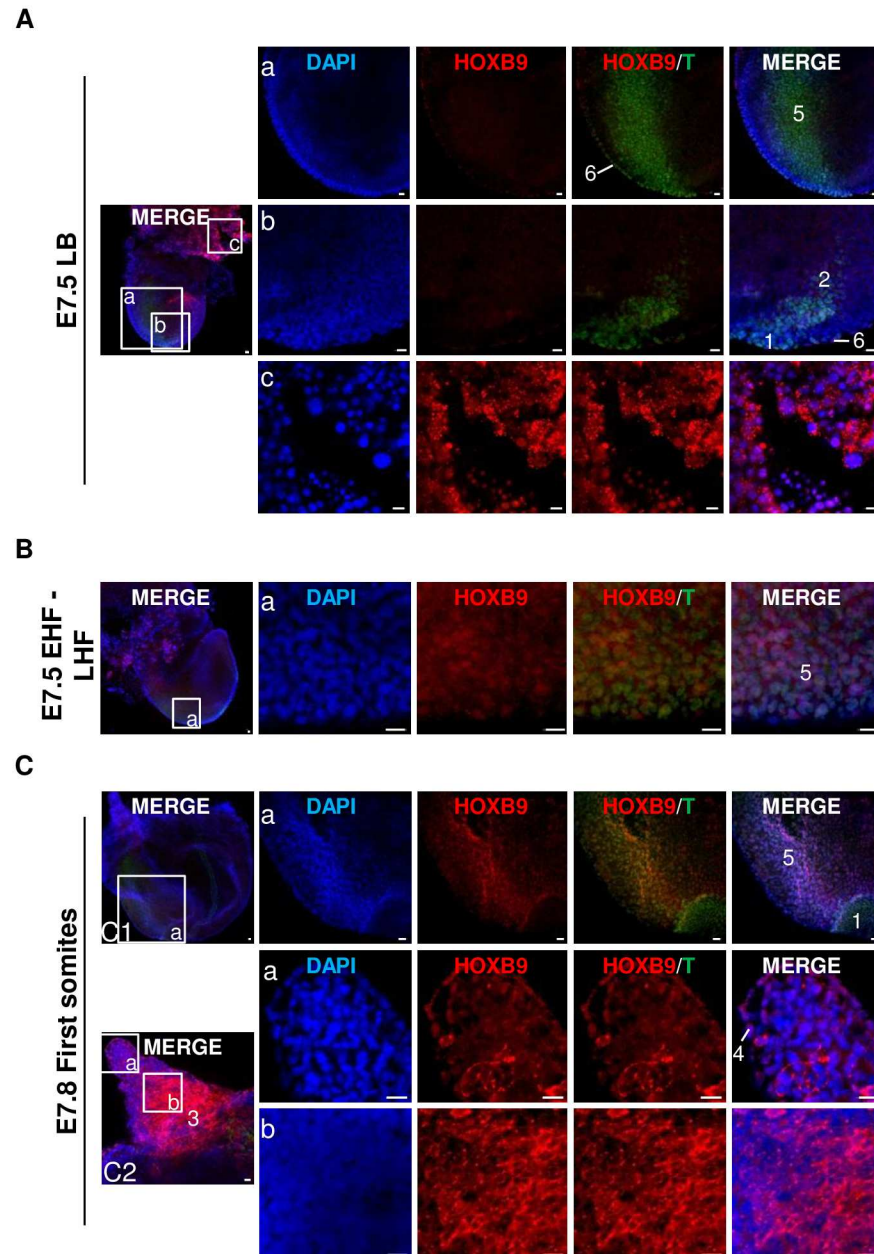


Fig 6. Mouse HOXB9 protein distribution in *in vivo* peri-gastrulating embryos: E7.5 and E7.8. A-C: Whole-mount immunofluorescence. **(A)** E7.5 late allantoic bud stage (LB). **(B)** E7.5 early headfold—late headfold stage (EHF—LHF). **(C)** E7.8 first somites stage. Zoom on allantois (**C2**). 1. node; 2. notochord; 3. allantois; 4. mesothelium of the allantois; 5. primitive streak; 6. embryonic visceral endoderm. Nuclei: Blue; HOXB9: Red; T: Green. Representative confocal Z-section. Scale bar = 20 μ m.

doi:10.1371/journal.pone.0165898.g006

tend to be more cuboidal and columnar with a more vacuolated cytoplasm when localized close to ExVE [68, 76]. The flattened cells of VE presented both cytoplasmic and nuclear HOXB9 localizations (Fig 5B3—section b—yellow arrows), while the cuboidal (Fig 5B2—section a—yellow arrowheads) and the more columnar (Fig 5B3—section a—yellow asterisk) cells showed HOXB9 localization in apical vacuoles similar to the one observed in E5.5. Finally, some VE cells located at the embryonic side opposite to primitive streak (Fig 5B2—section a) showed strong cytoplasmic HOXB9 signal (Fig 5B2—section b and Fig 5B3—section a—blue arrow), as opposed to the remaining VE. We thus hypothesized that these cells corresponded to the anterior visceral endoderm (AVE). A co-staining was therefore performed with CER-1, a secreted protein expressed by AVE cells [45]. The HOXB9 cytoplasmic signal in these cells did indeed co-localize with CER-1, confirming HOXB9 expression in AVE (Fig 5B4).

At the LB stage, HOXB9 protein distribution was similar to that observed in E6.5 embryos (Fig 6A). Both the node (formed at the anterior end of primitive streak—[50]) and the forming notochord (mesodermal median axis under the epiblast—[32]) were negative with regard to HOXB9 staining (Fig 6A—section b).

At the EHF-LHF stages, changes in immunostaining only appeared at the level of primitive streak where HOXB9 started to be expressed mainly in nuclei (Fig 6B).

At E7.8, stage characterized by the presence of somites, HOXB9 staining was more apparent in cells of primitive streak compared to EHF—LHF stage (Fig 6C1). Moreover, signal associated to HOXB9 was also present in the allantois (Fig 6C2). HOXB9 subcellular localization was nuclear in inner cells of the distal part of allantois and in the mesothelium (Fig 6C2—section a). Conversely, the signal was more intense and mainly cytoplasmic in the inner cells of the proximal region (Fig 6C2—section b). HOXB9 expression in allantois was already seen in EHF—LHF embryos.

To summarize, from E5.5 to E7.8, HOXB9 present a spatially-restricted and dynamic protein pattern in mouse embryos. HOXB9 expression is limited to trophoblast, PrE and its derivatives, and allantois cells. Modifications in the subcellular localization are also observed. The most striking feature of HOXB9 expression being (1) the progressive disappearance of the staining in epiblast cells and its reappearance in primitive streak once gastrulation had well progressed at the EHF—LHF stage, (2) the localization of HOXB9 at apical vacuoles in VE cells, (3) the association of HOXB9 with vesicles in trophoblast cells and (4) the cytoplasmic distribution of HOXB9 in AVE.

Distribution of bovine HOXB9 is ubiquitous in peri-gastrulating embryos and shares similarities with mouse HOXB9 distribution

In order to determine whether the mouse HOXB9 expression pattern was conserved in mammalian species around gastrulation, bovine embryos produced *in vivo* at stages D14 to D18 were examined. D14 (N = 2) and D17 (N = 2) embryos were co-stained with CDX2 to highlight trophoblastic cells [77], while D15 (N = 1) and D18 (N = 1) embryos were co-stained with VIMENTIN (VIM) and DLX3 to localize embryonic and extra-embryonic mesoderm cells [16, 52, 56] or trophoblastic cells [42], respectively.

Contrary to the restricted expression observed in peri-gastrulation mouse embryos, distribution of HOXB9 was largely ubiquitous in the bovine (Fig 7). Embryos examined at D14-15 had initiated gastrulation. Their shape appeared tubular and they displayed a completely formed primitive endoderm, while polar TE cells had disappeared, as expected [31]. At this stage, despite the presence of HOXB9 in all tissues, it is interesting to note that epiblast cells displayed a weaker staining than TE cells and presented homogeneous distribution between cells, as observed in D11 embryos (Fig 7A). Moreover, HOXB9 was mainly localized in the

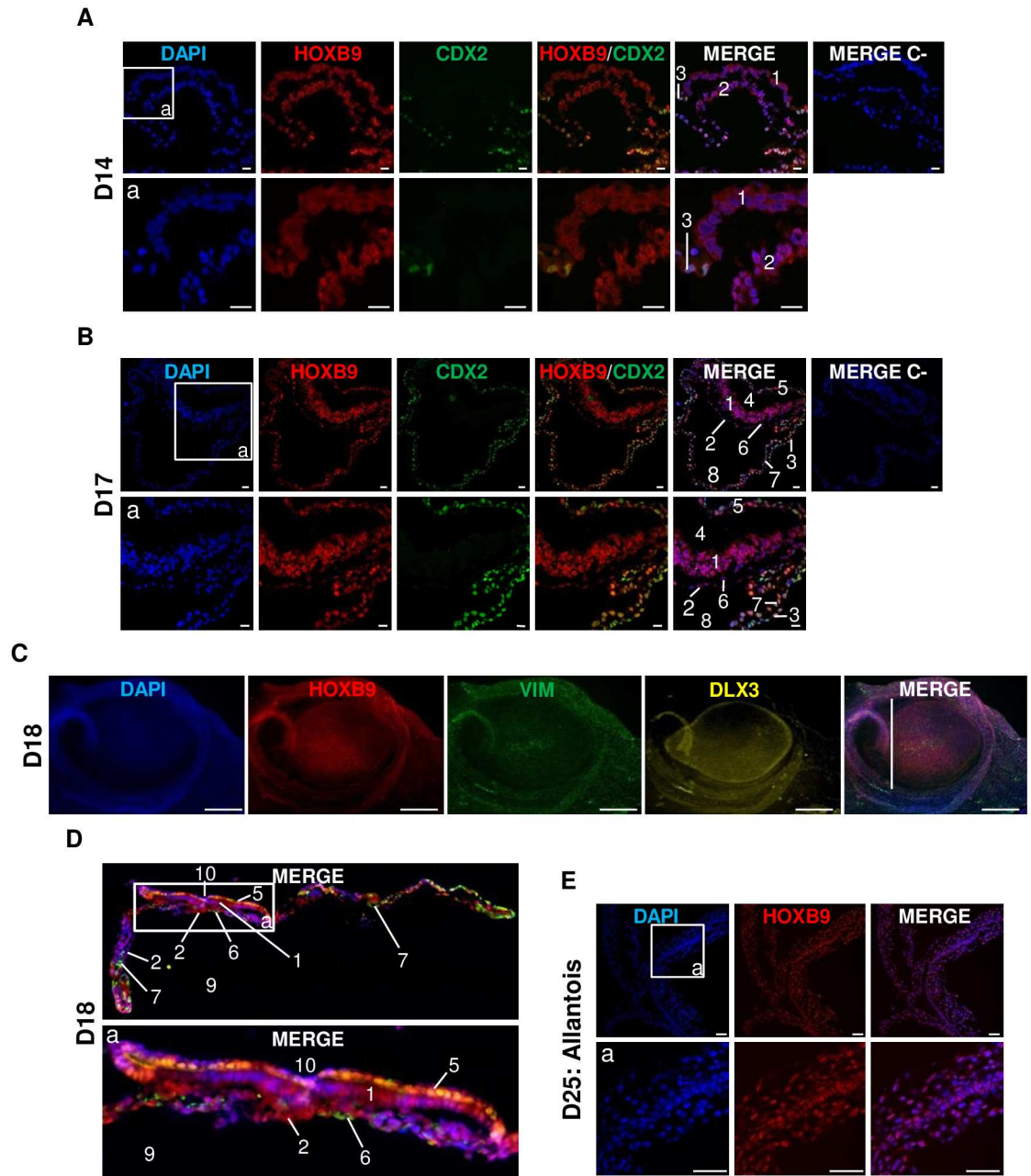


Fig 7. Distribution of bovine HOXB9 protein in *in vivo* peri-gastrulating embryos. **A, B:** Immunohistochemistry on D14 (**A**) and D17 (**B**) embryos. Merge C-: Negative control without primary antibody. Representative confocal Z-section. Scale bar = 20 μ m. **C, D:** Whole-mount immunofluorescence on D18 embryos (**C**) followed by immunohistochemistry (**D**). The localization of the sectioning is indicated by the white line in **C**. Epifluorescence images (**C**) and confocal Z-section (**D**). Scale bar = 500 μ m. **E:** Immunohistochemistry on allantois from D25 embryos. Representative confocal Z-section. Scale bar = 20 μ m. Nuclei: Blue; HOXB9: Red; CDX2/VIMENTIN: Green; DLX3: Yellow. 1. epiblast; 2. primitive endoderm; 3. mural trophoblast; 4. amniotic cavity; 5. amniotic wall; 6. embryonic mesoderm; 7. extra-embryonic mesoderm; 7 + 3 = chorion; 8. coelom; 9. yolk sac cavity; 7 + 2 = yolk sac wall; 10. primitive streak.

doi:10.1371/journal.pone.0165898.g007

nucleus of mural trophoblast cells, although a fainter cytoplasmic staining was also present. Likewise, PrE cells shared a strong nuclear and weaker cytoplasmic HOXB9 immunoreactivity.

At stages D17-18, epiblast cells presented intense HOXB9 staining in the nucleus and fainter staining in the cytoplasm (Fig 7B-7D). Trophoblast cells remained well stained, as did PrE

(extra-embryonic endoderm) cells. The amnion, which was positive for both CDX2 (Fig 7B) and DLX3 (Fig 7D), displayed the same HOXB9 pattern as trophoblast cells. The parietal extra-embryonic mesoderm was positive for HOXB9 and CDX2 as well (Fig 7B). Finally, all cells of the allantois of D25 embryos presented strong nuclear HOXB9 staining (Fig 7E), similar to that observed for the innermost cells of the distal part the mouse allantois.

To sum up, HOXB9 is ubiquitously expressed in the bovine embryos. The abundance of HOXB9 is reduced in epiblast cells of D14-15 embryos compared to trophoblast cells in a nearly homogeneous way between epiblast cells, as observed for D11 embryos. Thereafter, HOXB9 distribution evolves into the strong nuclear staining observed in D17-18 embryos. Similarly to the mouse embryos, HOXB9 expression is downregulated in bovine epiblast cells before gastrulation and again increase at later stages. In addition, the presence of HOXB9 proteins in TE, allantois and in PrE and its derivatives seems to be conserved between the two species.

Discussion

The general objective of this work was to study the localization of HOXB9 during oocyte maturation and early embryonic development (until peri-gastrulating stage) in mammals. Within this framework, we assessed for the first time the presence and the subcellular localization of the protein at specific time points during this period and performed a comparative analysis of HOXB9 distribution in the mouse and bovine. A schematic comparison of the subcellular distribution of HOXB9 in mouse and bovine oocytes and in the different cell types of early embryo until the peri-gastrulation period is shown in Fig 8. In summary, we demonstrated that (1) HOXB9 distribution is conserved in the two species in oocytes and from the zygote to the blastocyst stage, with a mainly nuclear localization; (2) at the blastocyst stage, in both species, nuclear HOXB9 is more abundant in TE than in ICM where its abundance decreases in a non-uniform way during blastocyst expansion; (3) in the bovine, a strong nuclear staining is observed in the forming PrE, while signal was concomitantly reduced in epiblast cells; (4) in mouse pre- and post-gastrulating embryos, HOXB9 is restricted to the trophoblast, PrE and derivatives, and allantois, presenting various surprising intra-cellular localization including the apical vacuoles of VE cells (from E5.5), the vesicles of trophoblast cells (from E6.5) and the cytoplasm of AVE cells; (5) during gastrulation, bovine epiblast cells re-acquire a strong HOXB9 signal in nuclei, while in the mouse, HOXB9, which was almost extinct in the epiblast, appears turned on in primitive streak.

Overall, throughout the developmental period studied, HOXB9 was found in the nucleus and cytoplasm. Of course, nuclear HOXB9 localization could be linked to the well described transcription factor role of HOXB9. However, HOXB9 could also be implicated in other processes taking place in the nucleus [7], such as DNA repair [78]. The cytoplasmic localization suggests possible non-transcriptional functions of the protein. In the cytoplasm, HOXB9 could act as translation regulator, as it has been demonstrated for HOXA9 [79]. Changes in HOXB9 distribution between the nucleus and cytoplasm could also reflect a way to regulate its transcriptional activity, as it has previously been reported for HOXA2 [80].

From the immature fully grown oocyte to the morula stage, HOXB9 protein was detected in all cells with a strong nuclear localization, both in the mouse and bovine. Our study is thus in accordance with previously published mRNA profiles showing the presence of maternal transcripts up to MET and *de novo* transcription from the embryonic genome afterwards [24]. However, our study could not differentiate between the maternal or embryonic origin of the protein. It is therefore not known if maternal HOXB9 is still present after MET, as already demonstrated for other proteins such as OCT4, CDX2 or SOX2 [81–83].

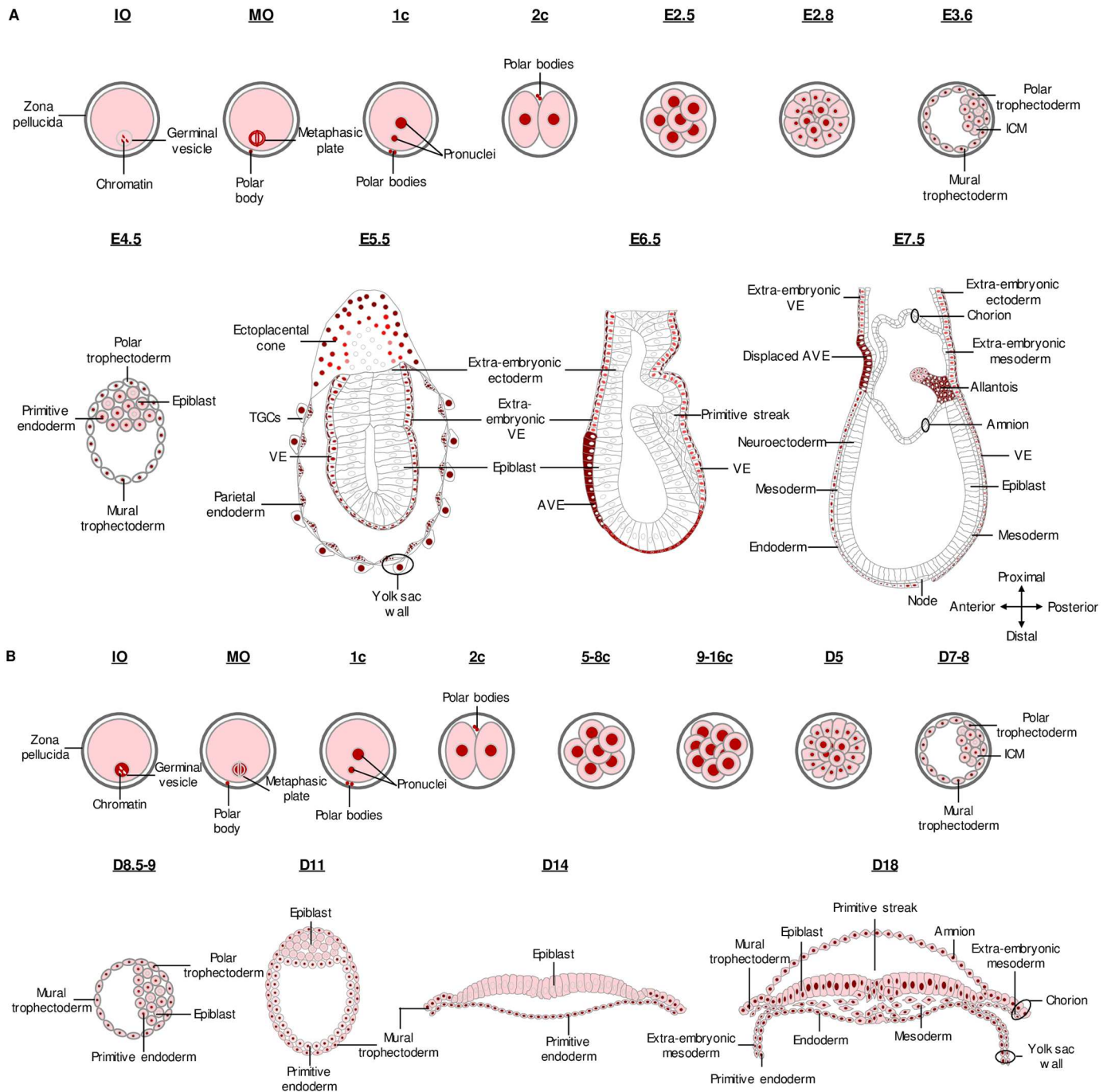


Fig 8. Schematic summary of the HOXB9 protein distribution in mouse (A) and bovine (B) early embryonic development. Immature oocyte (IO); Mature oocyte (MO); 1-cell embryo (1c); 2-cell embryo (2c); 5- to 8-cell embryo (5–8c); 9- to 16-cell embryo (9–16c); Inner Cell Mass (ICM); Visceral endoderm (VE); Trophoblastic Giant Cells (TGCs); Anterior Visceral Endoderm (AVE). Tissues represented without nucleus in E7.5 embryos were not examined in details.

doi:10.1371/journal.pone.0165898.g008

This period of development is marked by important events such as oocyte maturation, fertilization and EGA, which occurs between the 5- to 8-cell and the 9- to 16-cell stage in the bovine and before the 2-cell stage in the mouse [28, 84]. HOXB9 might thus play a role in the control of EGA but could also regulate the very few genes that are transcribed at the earliest stages.

Several genes have been shown to be directly or indirectly regulated by HOXB9 [47, 85–87] and, for some of them, are known to be expressed in oocytes and/or early embryos and could potentially act downstream of HOXB9 in such context. For example, HOXB9 is known to directly regulate *TGF-β2* transcription and the TGF-β/SMAD pathway is crucial for the bidirectional communication between the oocyte and the surrounding granulosa/cumulus cells [88].

At the blastocyst stage, a progressive change was observed in HOXB9 subcellular localization in both species. While a strong nuclear staining was still observed in TE cells, the nuclear staining heterogeneously decreased between nuclei of ICM cells. This is in accordance with the study by Ozawa et al. [89], which reported a trend towards a greater *HOXB9* expression in TE cells compared to ICM cells in bovine blastocysts produced *in vitro*. Conversely, the study of Hosseini et al. [90] identified the *HOXB9* gene as exclusively expressed in ICM of bovine blastocysts produced *in vivo*. This discrepancy between *in vitro* and *in vivo* embryos remains difficult to reconcile all the more so as we observed the same pattern of HOXB9 protein distribution both in *in vivo* and in *in vitro* blastocysts.

Since HOXB9 is mainly nuclear in TE, it is likely to act as a transcription factor during establishment and maintenance of TE. Interestingly, many direct or indirect HOXB9 target genes identified in distinct contexts [47, 85–87] are expressed in TE. AMPHIREGULIN is an EGF-like peptide involved in TE cell proliferation in the mouse and pig [91, 92]. In the pig, AMPHIREGULIN expression profile is similar to the one observed for the bovine *HOXB9* [92]. TGF-β2, another HOXB9 target, is detected in the mouse [93, 94] and pig [95] TE cells and is present in the fetal and maternal components of the bovine placenta [96, 97]. β-CATENIN and E-CADHERIN are present in the mouse and bovine from oocytes to blastocysts [98–100]. Together, they play a crucial role during morula compaction and TE formation [101–105]. N-CAM expression has been observed in bovine blastocysts (D. Paul and L. Bridoux, personal communication) and the protein, known to mediate cell adhesion, is present in murine TE cells [106]. Moreover, HOXB9 co-localized with CDX2, a validated *HOXB9* regulator involved in TE lineage determination [58, 107–109], in TE of both species and in a TE-derived bovine cell line (CT-1 cells—S1 File). Considering the co-localization of CDX2 and HOXB9 in TE cells, the impact of a *CDX2* knock-down on *HOXB9* mRNA in CT-1 cells was assayed (S1 File). *CDX2* knock-down in CT-1 cells did not appear to impact *HOXB9* mRNA relative expression.

Inner cell mass of E3.5 mouse and D7 bovine blastocysts is a mosaic of PrE and epiblast progenitors that will completely segregate at the late blastocyst stage. HOXB9 protein expression was heterogeneous in ICM of mouse (E3.6) and bovine blastocysts (from D7.5). However, this did not systematically correlate with the presence of the PrE markers (GATA6 or GATA4). In the bovine, once the PrE and epiblast segregation occurs, PrE cells strongly expressed HOXB9, while its expression was reduced but homogeneous in epiblast cells, suggesting an involvement of HOXB9 in bovine PrE formation. Although E4.5 mouse embryos analyzed in this study did not display a PrE, the detection of HOXB9 in PrE derivatives at later stages suggested a similar pattern in both species. Moreover, as was the case in the bovine, mouse HOXB9 protein was down-regulated in epiblast cells from E5.5 embryos.

The nuclear HOXB9 observed in TE cells persisted in trophoblast cells of both species at later stages. This observation is in accordance with *HOX* gene expression, including *HOX9*, reported in the mouse and human placenta [110–113]. In trophoblast cells, HOXB9 could contribute to the implantation process (reviewed in [114, 115]) by promoting the epithelial-to-mesenchymal transition (EMT), angiogenesis, cell migration and invasion (mouse) through the regulation of angiogenic factors and *TGF-β2*, as evidenced in cancers [47, 85–87]. Moreover, in a subset of superficial trophoblast cells from E6.5 mouse embryos, HOXB9 was observed in association with cytoplasmic vesicles. Trophoblast cells release exosomes that play

important roles in the intercellular communication that contributes to placentation and to the development of maternal-fetal exchanges [116]. Furthermore, exosomes deriving from human cancer cells are shown to contain HOX proteins [117] and facilitate angiogenesis [118]. It is therefore possible that HOXB9 is released from trophoblast cells in exosomes and participates in the placentation process in this species. Due to the late placentation in the bovine (D21), no bovine trophoblast cells corresponding to the timing of implantation could be observed.

The localization of HOXB9 protein in mouse peri-gastrulating embryos and E12.5 embryos coincided with expression patterns determined by *in situ* hybridization, with the exception of the staining observed in PrE derivatives, which was not previously reported [8, 12–14]. Localization of HOXB9 in PrE derivatives was observed both in the mouse and bovine. Visceral endoderm influences the differentiation and development of blood islands and vessels in the underlying extra-embryonic mesoderm and coordinates blood cell differentiation [70]. HOXB9 could be involved in both processes, via the induction of angiogenic factors expression but also through an active role in embryonic erythropoiesis, as previously suggested [10].

Mouse HOXB9 co-localized with maternal IgGs within or associated to VE apical vacuoles at E5.5. Prior to the formation of a functional placenta in mouse embryo (at E10), nutrients as well as signaling molecules are endocytosed by VE cells and the resulting early endosomes deliver their content to apical vacuoles through microautophagy [119]. This process is essential for the embryo as shown by the developmental defects, particularly at the gastrulation step, observed in loss of function experiments of proteins involved in VE cell endocytosis [120–122]. On one hand, the presence of HOXB9 within VE apical vacuoles could reflect the presence of extracellular HOXB9 cooperating with signaling pathways to control the embryo patterning. Whether vacuole-associated HOXB9 is of maternal and/or embryonic origin has to be determined. On the other hand, if HOXB9 is associated with the cytoplasmic interface of apical vacuoles, HOXB9 could be originating from VE. In both situations, the association of HOXB9 with apical vacuoles might be linked to the modulation of signaling pathways and/or could represent a way of regulating HOXB9 activity.

A prominent HOXB9 staining was observed in the cytoplasm of mouse AVE, which is an early organizer that specifies the anterior-posterior axis of the embryo [70]. The cytoplasmic localization of HOXB9 in AVE could reflect a regulation of its transcriptional activity or its function as a translation regulator.

HOXB9 was expressed in the allantois in the mouse and bovine. Scotti and Kmita [123] previously demonstrated a *Hoxa10-Hoxa13* expression in the allantois of E7.5 and E8.5 mouse embryos, which is required for proper expansion of the fetal vasculature in the placenta. Ledgard et al. [15] and Hue et al. [16] also reported *HOX* expression in the bovine allantois. In the mouse, CDX2 was reported to be essential for allantoic growth and chorio-allantoic fusion [124]. HOXB9 could therefore act downstream of CDX2 in the control of allantois cell proliferation and in the development of a functional placenta.

As previously mentioned, *Hoxb9*^{-/-} mutant animals are viable and fertile indicating that maternal and zygotic *Hoxb9* loss of function is not embryo lethal. However, no exhaustive studies have so far been performed on *Hoxb9*^{-/-} mutant animals with regard to ovulation/maturation rates, littermate size or early development and implantation rates of their offspring. Moreover, the absence of a phenotype could be due to the presence of other HOX proteins, including HOX9 proteins, whose expression has previously been detected during early embryonic development [24], that could be functionally redundant. In addition, it is likely that HOXB9 acts in concert with other actors to control early embryonic development. Although not critical for oocyte/embryo development, as highlighted by loss of function studies, the involvement of maternal and/or zygotic HOXB9 in one or several of these processes cannot be ruled out. In order to address the function of both maternal and zygotic HOXB9, a knock-

down approach by RNA interference in bovine oocytes, zygotes or trophectoderm cell line (CT-1 cells) was attempted (S1 File). Unfortunately, experiments did not significantly impact the protein abundance and conclusions on the role(s) maternal and zygotic HOXB9 could play in early embryonic development could not be drawn.

In conclusion, from the HOXB9 protein profile established in this exhaustive study, we could hypothesize a previously unsuspected involvement of HOXB9 in mammalian early embryonic development and, more specifically, in cell lineage differentiation, embryo patterning, allantois development and implantation.

Supporting Information

S1 File. HOXB9 functional analyses during bovine oocyte maturation and early embryo development.

(DOCX)

Acknowledgments

We gratefully acknowledge the team of Professor Schellander from the University of Bonn and in particular Franca Rings and David Tesfaye for the training in microinjection and the fruitful discussions about siRNA. We are very grateful to Gene diffusion (Douai, France), especially Gérard Bernard and Luc Liégeois, for the gift of D11 bovine embryos produced *in vivo*. We also wish to thank the Awé (Belgium), particularly Christophe Boccart, for the D7 bovine blastocysts produced *in vivo*. We express our gratitude to Niel Talbot (U.S. Department of Agriculture, Beltsville, USA) for providing the CT-1 cells and for all his advice to establish and maintain the CT-1 cells culture. We thank Deneen Wellik from University of Michigan (Ann Arbor, USA) for generously providing mouse *Hox9* expression vectors and *Hoxb9*^{-/-} E12.5 embryos, for her interest in our research and for all the discussions about our project. Our appreciation is extended to Pierre Courtois and Patrick Van Der Smissen from the Université catholique de Louvain (Woluwe-Saint-Lambert, Belgium) for the access to microscope facilities and for thorough advice. We also thank Sébastien Mauën (Celyad, Mont-Saint-Guibert, Belgium) for his assistance in developing an analytical method for images quantification. We acknowledge the IMABIOL platform and the SMCS from the Université catholique de Louvain (Louvain-la-Neuve, Belgium) for confocal microscopy support and for the statistical analysis, respectively. The authors also thank the Cochin Institute Imaging facility and the HistIM platform (Paris, France). We are very grateful to all members of the Animal Molecular and Cellular Biology team for their assistance in embryo production and Marie-Anne Mauclet for her help with administrative procedures. The authors like to thank Jacqueline Deschamps from Hubrecht Institut (Utrecht, Netherlands) for useful discussions of the results and Françoise Gofflot from Université catholique de Louvain for stimulating discussions. We acknowledge Marc Pirson for English editing. CS holds a FRIA fellowship from the FNRS (Belgium).

Author Contributions

Conceptualization: CS RR ID.

Formal analysis: CS DP LB.

Funding acquisition: RR ID.

Investigation: CS DP LB AJ SD.

Methodology: CS DP SD IH RR ID.

Project administration: RR ID.

Resources: AJ SD IH.

Supervision: RR ID.

Visualization: CS DP LB.

Writing – original draft: CS.

Writing – review & editing: CS IH RR ID.

References

1. Lappin TR, Grier DG, Thompson A, Halliday HL. HOX genes: seductive science, mysterious mechanisms. *The Ulster medical journal*. 2006; 75(1):23–31. PMID: [16457401](#); PubMed Central PMCID: PMC1891803.
2. Mallo M, Wellik DM, Deschamps J. Hox genes and regional patterning of the vertebrate body plan. *Developmental biology*. 2010; 344(1):7–15. doi: [10.1016/j.ydbio.2010.04.024](#) PMID: [20435029](#); PubMed Central PMCID: PMCPMC2909379.
3. Wellik DM. Hox genes and kidney development. *Pediatr Nephrol*. 2011; 26(9):1559–65. doi: [10.1007/s00467-011-1902-1](#) PMID: [21553325](#).
4. Xu B, Wellik DM. Axial Hox9 activity establishes the posterior field in the developing forelimb. *Proceedings of the National Academy of Sciences of the United States of America*. 2011; 108(12):4888–91. doi: [10.1073/pnas.1018161108](#) PMID: [21383175](#); PubMed Central PMCID: PMCPMC3064354.
5. Foronda D, de Navas LF, Garaulet DL, Sanchez-Herrero E. Function and specificity of Hox genes. *The International journal of developmental biology*. 2009; 53(8–10):1404–19. doi: [10.1387/ijdb.072462df](#) PMID: [19247930](#).
6. Rezsohazy R, Saurin AJ, Maurel-Zaffran C, Graba Y. Cellular and molecular insights into Hox protein action. *Development*. 2015; 142(7):1212–27. doi: [10.1242/dev.109785](#) PMID: [25804734](#).
7. Rezsohazy R. Non-transcriptional interactions of Hox proteins: inventory, facts, and future directions. *Developmental dynamics: an official publication of the American Association of Anatomists*. 2014; 243(1):117–31. doi: [10.1002/dvdy.24060](#) PMID: [24115586](#).
8. Chen F, Capecchi MR. Targeted mutations in *hoxa-9* and *hoxb-9* reveal synergistic interactions. *Developmental biology*. 1997; 181(2):186–96. doi: [10.1006/dbio.1996.8440](#) PMID: [9013929](#).
9. McIntyre DC, Rakshit S, Yallowitz AR, Loken L, Jeannotte L, Capecchi MR, et al. Hox patterning of the vertebrate rib cage. *Development*. 2007; 134(16):2981–9. doi: [10.1242/dev.007567](#) PMID: [17626057](#).
10. Magli MC, Largman C, Lawrence HJ. Effects of HOX homeobox genes in blood cell differentiation. *Journal of cellular physiology*. 1997; 173(2):168–77. doi: [10.1002/\(SICI\)1097-4652\(199711\)173:2<168::AID-JCP16>3.0.CO;2-C](#) PMID: [9365517](#).
11. Chen F, Capecchi MR. Paralogous mouse Hox genes, *Hoxa9*, *Hoxb9*, and *Hoxd9*, function together to control development of the mammary gland in response to pregnancy. *Proceedings of the National Academy of Sciences of the United States of America*. 1999; 96(2):541–6. PMID: [9892669](#); PubMed Central PMCID: PMC15172.
12. Chambeyron S, Da Silva NR, Lawson KA, Bickmore WA. Nuclear re-organisation of the *Hoxb* complex during mouse embryonic development. *Development*. 2005; 132(9):2215–23. doi: [10.1242/dev.01813](#) PMID: [15829525](#).
13. Conlon RA, Rossant J. Exogenous retinoic acid rapidly induces anterior ectopic expression of murine *Hox-2* genes in vivo. *Development*. 1992; 116(2):357–68. PMID: [1363087](#).
14. van Rooijen C, Simmini S, Bialecka M, Neijts R, van de Ven C, Beck F, et al. Evolutionarily conserved requirement of *Cdx* for post-occipital tissue emergence. *Development*. 2012; 139(14):2576–83. doi: [10.1242/dev.079848](#) PMID: [22675207](#).
15. Ledgard AM, Lee RS, Peterson AJ. Expression of genes associated with allantois emergence in ovine and bovine conceptuses. *Molecular reproduction and development*. 2006; 73(9):1084–93. doi: [10.1002/mrd.20532](#) PMID: [16804885](#).
16. Hue I, Evain-Brion D, Fournier T, Degrelle SA. Primary Bovine Extra-Embryonic Cultured Cells: A New Resource for the Study of In Vivo Peri-Implanting Phenotypes and Mesoderm Formation. *PloS one*. 2015; 10(6):e0127330. doi: [10.1371/journal.pone.0127330](#) PMID: [26070137](#).

17. Mamo S, Mehta JP, McGettigan P, Fair T, Spencer TE, Bazer FW, et al. RNA sequencing reveals novel gene clusters in bovine conceptuses associated with maternal recognition of pregnancy and implantation. *Biology of reproduction*. 2011; 85(6):1143–51. doi: [10.1095/biolreprod.111.092643](https://doi.org/10.1095/biolreprod.111.092643) PMID: [21795669](https://pubmed.ncbi.nlm.nih.gov/21795669/).
18. Adjaye J, Monk M. Transcription of homeobox-containing genes detected in cDNA libraries derived from human unfertilized oocytes and preimplantation embryos. *Molecular human reproduction*. 2000; 6(8):707–11. PMID: [10908280](https://pubmed.ncbi.nlm.nih.gov/10908280/).
19. Gao Y, Hyttel P, Hall VJ. Regulation of H3K27me3 and H3K4me3 during early porcine embryonic development. *Molecular reproduction and development*. 2010; 77(6):540–9. doi: [10.1002/mrd.21180](https://doi.org/10.1002/mrd.21180) PMID: [20422712](https://pubmed.ncbi.nlm.nih.gov/20422712/).
20. Huntriss J, Hinkins M, Picton HM. cDNA cloning and expression of the human NOBOX gene in oocytes and ovarian follicles. *Molecular human reproduction*. 2006; 12(5):283–9. doi: [10.1093/molehr/gal035](https://doi.org/10.1093/molehr/gal035) PMID: [16597639](https://pubmed.ncbi.nlm.nih.gov/16597639/).
21. Kageyama S, Gunji W, Nakasato M, Murakami Y, Nagata M, Aoki F. Analysis of transcription factor expression during oogenesis and preimplantation development in mice. *Zygote*. 2007; 15(2):117–28. doi: [10.1017/S096719940700411X](https://doi.org/10.1017/S096719940700411X) PMID: [17462104](https://pubmed.ncbi.nlm.nih.gov/17462104/).
22. Ota T, Asahina H, Park SH, Huang Q, Minegishi T, Auersperg N, et al. HOX cofactors expression and regulation in the human ovary. *Reproductive biology and endocrinology: RB&E*. 2008; 6:49. doi: [10.1186/1477-7827-6-49](https://doi.org/10.1186/1477-7827-6-49) PMID: [18973687](https://pubmed.ncbi.nlm.nih.gov/18973687/); PubMed Central PMCID: [PMC2585084](https://pubmed.ncbi.nlm.nih.gov/PMC2585084/).
23. Ota T, Choi KB, Gilks CB, Leung PC, Auersperg N. Cell type- and stage-specific changes in HOXA7 protein expression in human ovarian folliculogenesis: possible role of GDF-9. *Differentiation; research in biological diversity*. 2006; 74(1):1–10. doi: [10.1111/j.1432-0436.2006.00053.x](https://doi.org/10.1111/j.1432-0436.2006.00053.x) PMID: [16466395](https://pubmed.ncbi.nlm.nih.gov/16466395/).
24. Paul D, Bridoux L, Rezsöházy R, Donnay I. HOX genes are expressed in bovine and mouse oocytes and early embryos. *Molecular reproduction and development*. 2011; 78(6):436–49. doi: [10.1002/mrd.21321](https://doi.org/10.1002/mrd.21321) PMID: [21567651](https://pubmed.ncbi.nlm.nih.gov/21567651/).
25. Ponsuksili S, Wimmers K, Adjaye J, Schellander K. Expression of homeobox-containing genes in cDNA libraries derived from cattle oocytes and preimplantation stage embryo. *Molecular reproduction and development*. 2001; 60(3):297–301. doi: [10.1002/mrd.1091](https://doi.org/10.1002/mrd.1091) PMID: [11599040](https://pubmed.ncbi.nlm.nih.gov/11599040/).
26. Verlinsky Y, Morozov G, Gindilis V, Strom CM, Freidin M, Rechitsky S, et al. Homeobox gene expression in human oocytes and preembryos. *Molecular reproduction and development*. 1995; 41(2):127–32. doi: [10.1002/mrd.1080410202](https://doi.org/10.1002/mrd.1080410202) PMID: [7654365](https://pubmed.ncbi.nlm.nih.gov/7654365/).
27. Villaescusa JC, Verrotti AC, Ferretti E, Farookhi R, Blasi F. Expression of Hox cofactor genes during mouse ovarian follicular development and oocyte maturation. *Gene*. 2004; 330:1–7. doi: [10.1016/j.gene.2004.01.024](https://doi.org/10.1016/j.gene.2004.01.024) PMID: [15087118](https://pubmed.ncbi.nlm.nih.gov/15087118/).
28. Li L, Lu X, Dean J. The maternal to zygotic transition in mammals. *Molecular aspects of medicine*. 2013; 34(5):919–38. doi: [10.1016/j.mam.2013.01.003](https://doi.org/10.1016/j.mam.2013.01.003) PMID: [23352575](https://pubmed.ncbi.nlm.nih.gov/23352575/); PubMed Central PMCID: [PMC3669654](https://pubmed.ncbi.nlm.nih.gov/PMC3669654/).
29. Aoki F, Worrad DM, Schultz RM. Regulation of transcriptional activity during the first and second cell cycles in the preimplantation mouse embryo. *Developmental biology*. 1997; 181(2):296–307. doi: [10.1006/dbio.1996.8466](https://doi.org/10.1006/dbio.1996.8466) PMID: [9013938](https://pubmed.ncbi.nlm.nih.gov/9013938/).
30. Barnes FL, First NL. Embryonic transcription in in vitro cultured bovine embryos. *Molecular reproduction and development*. 1991; 29(2):117–23. doi: [10.1002/mrd.1080290205](https://doi.org/10.1002/mrd.1080290205) PMID: [1878221](https://pubmed.ncbi.nlm.nih.gov/1878221/).
31. Maddox-Hyttel P, Sinowatz F, Vejlsted M. *Essentials of domestic animal embryology*: Saunders Elsevier; 2010.
32. Nagy A, Gertsenstun M, Vintsrten K, Behringer R. *Manipulating the mouse embryo: a laboratory manual*. Third Edition ed. New York: Cold Spring Harbor Laboratory Press; 2003.
33. Donnay I, Faerge I, Grondahl C, Verhaeghe B, Sayoud H, Ponderato N, et al. Effect of prematuration, meiosis activating sterol and enriched maturation medium on the nuclear maturation and competence to development of calf oocytes. *Theriogenology*. 2004; 62(6):1093–107. doi: [10.1016/j.theriogenology.2003.12.019](https://doi.org/10.1016/j.theriogenology.2003.12.019) PMID: [15289049](https://pubmed.ncbi.nlm.nih.gov/15289049/).
34. Holm P, Booth PJ, Schmidt MH, Greve T, Callesen H. High bovine blastocyst development in a static in vitro production system using SOFaa medium supplemented with sodium citrate and myo-inositol with or without serum-proteins. *Theriogenology*. 1999; 52(4):683–700. doi: [10.1016/S0093-691X\(99\)00162-4](https://doi.org/10.1016/S0093-691X(99)00162-4) PMID: [10734366](https://pubmed.ncbi.nlm.nih.gov/10734366/).
35. George F, Daniaux C, Genicot G, Verhaeghe B, Lambert P, Donnay I. Set up of a serum-free culture system for bovine embryos: embryo development and quality before and after transient transfer. *Theriogenology*. 2008; 69(5):612–23. doi: [10.1016/j.theriogenology.2007.11.008](https://doi.org/10.1016/j.theriogenology.2007.11.008) PMID: [18242668](https://pubmed.ncbi.nlm.nih.gov/18242668/).

36. Cocero MJ, Sebastian AL, Barragan ML, Picazo RA. Differences on post-thawing survival between ovine morulae and blastocysts cryopreserved with ethylene glycol or glycerol. *Cryobiology*. 1996; 33(5):502–7. doi: [10.1006/cryo.1996.0053](https://doi.org/10.1006/cryo.1996.0053) PMID: [8893509](https://pubmed.ncbi.nlm.nih.gov/8893509/).
37. Richard C, Hue I, Gelin V, Neveux A, Campion E, Degrelle SA, et al. Transcervical collection of bovine embryos up to Day 21: an 8-year overview. *Theriogenology*. 2015; 83(7):1101–9. doi: [10.1016/j.theriogenology.2014.12.005](https://doi.org/10.1016/j.theriogenology.2014.12.005) PMID: [25662200](https://pubmed.ncbi.nlm.nih.gov/25662200/).
38. Guillomot M, Taghouti G, Constant F, Degrelle S, Hue I, Chavatte-Palmer P, et al. Abnormal expression of the imprinted gene Phlda2 in cloned bovine placenta. *Placenta*. 2010; 31(6):482–90. doi: [10.1016/j.placenta.2010.03.004](https://doi.org/10.1016/j.placenta.2010.03.004) PMID: [20381142](https://pubmed.ncbi.nlm.nih.gov/20381142/).
39. Barrios-Rodiles M, Brown KR, Ozdamar B, Bose R, Liu Z, Donovan RS, et al. High-throughput mapping of a dynamic signaling network in mammalian cells. *Science*. 2005; 307(5715):1621–5. doi: [10.1126/science.1105776](https://doi.org/10.1126/science.1105776) PMID: [15761153](https://pubmed.ncbi.nlm.nih.gov/15761153/).
40. Blij S, Frum T, Akyol A, Fearon E, Ralston A. Maternal Cdx2 is dispensable for mouse development. *Development*. 2012; 139(21):3969–72. doi: [10.1242/dev.086025](https://doi.org/10.1242/dev.086025) PMID: [22992952](https://pubmed.ncbi.nlm.nih.gov/22992952/); PubMed Central PMCID: [PMC3472595](https://pubmed.ncbi.nlm.nih.gov/PMC3472595/).
41. Goossens K, Vandaele L, Wydooghe E, Thys M, Dewulf J, Peelman LJ, et al. The importance of adequate fixation for immunofluorescent staining of bovine embryos. *Reproduction in domestic animals = Zuchthygiene*. 2011; 46(6):1098–103. doi: [10.1111/j.1439-0531.2011.01770.x](https://doi.org/10.1111/j.1439-0531.2011.01770.x) PMID: [21366723](https://pubmed.ncbi.nlm.nih.gov/21366723/).
42. Degrelle SA, Murthi P, Evain-Brion D, Fournier T, Hue I. Expression and localization of DLX3, PPARG and SP1 in bovine trophoblast during binucleated cell differentiation. *Placenta*. 2011; 32(11):917–20. doi: [10.1016/j.placenta.2011.08.014](https://doi.org/10.1016/j.placenta.2011.08.014) PMID: [21937107](https://pubmed.ncbi.nlm.nih.gov/21937107/).
43. Papanayotou C, Benhaddou A, Camus A, Perea-Gomez A, Jouneau A, Mezger V, et al. A novel nodal enhancer dependent on pluripotency factors and smad2/3 signaling conditions a regulatory switch during epiblast maturation. *PLoS biology*. 2014; 12(6):e1001890. doi: [10.1371/journal.pbio.1001890](https://doi.org/10.1371/journal.pbio.1001890) PMID: [24960041](https://pubmed.ncbi.nlm.nih.gov/24960041/); PubMed Central PMCID: [PMC4068991](https://pubmed.ncbi.nlm.nih.gov/PMC4068991/).
44. Plusa B, Piliszek A, Frankenberg S, Artus J, Hadjantonakis AK. Distinct sequential cell behaviours direct primitive endoderm formation in the mouse blastocyst. *Development*. 2008; 135(18):3081–91. doi: [10.1242/dev.021519](https://doi.org/10.1242/dev.021519) PMID: [18725515](https://pubmed.ncbi.nlm.nih.gov/18725515/); PubMed Central PMCID: [PMC2768606](https://pubmed.ncbi.nlm.nih.gov/PMC2768606/).
45. Hoshino H, Shioi G, Aizawa S. AVE protein expression and visceral endoderm cell behavior during anterior-posterior axis formation in mouse embryos: Asymmetry in OTX2 and DKK1 expression. *Dev Biol*. 2015; 402(2):175–91. doi: [10.1016/j.ydbio.2015.03.023](https://doi.org/10.1016/j.ydbio.2015.03.023) PMID: [25910836](https://pubmed.ncbi.nlm.nih.gov/25910836/).
46. Paul D, Sauvegarde C, Rezsöházy R, Donnay I. How to study HOX gene expression and function in mammalian oocytes and early embryos. *Methods in molecular biology*. 2014; 1196:19–36. doi: [10.1007/978-1-4939-1242-1_2](https://doi.org/10.1007/978-1-4939-1242-1_2) PMID: [25151155](https://pubmed.ncbi.nlm.nih.gov/25151155/).
47. Shrestha B, Ansari KI, Bhan A, Kasiri S, Hussain I, Mandal SS. Homeodomain-containing protein HOXB9 regulates expression of growth and angiogenic factors, facilitates tumor growth in vitro and is overexpressed in breast cancer tissue. *The FEBS journal*. 2012; 279(19):3715–26. doi: [10.1111/j.1742-4658.2012.08733.x](https://doi.org/10.1111/j.1742-4658.2012.08733.x) PMID: [22863320](https://pubmed.ncbi.nlm.nih.gov/22863320/); PubMed Central PMCID: [PMC3445661](https://pubmed.ncbi.nlm.nih.gov/PMC3445661/).
48. Graham A, Maden M, Krumlauf R. The murine Hox-2 genes display dynamic dorsoventral patterns of expression during central nervous system development. *Development*. 1991; 112(1):255–64. PMID: [1685115](https://pubmed.ncbi.nlm.nih.gov/1685115/).
49. Hunt P, Whiting J, Nonchev S, Sham MH, Marshall H, Graham A, et al. The branchial Hox code and its implications for gene regulation, patterning of the nervous system and head evolution. *Development*. 1991; Suppl 2:63–77. PMID: [1688181](https://pubmed.ncbi.nlm.nih.gov/1688181/).
50. Downs KM, Davies T. Staging of gastrulating mouse embryos by morphological landmarks in the dissecting microscope. *Development*. 1993; 118(4):1255–66. PMID: [8269852](https://pubmed.ncbi.nlm.nih.gov/8269852/).
51. Lu CC, Brennan J, Robertson EJ. From fertilization to gastrulation: axis formation in the mouse embryo. *Current opinion in genetics & development*. 2001; 11(4):384–92. PMID: [11448624](https://pubmed.ncbi.nlm.nih.gov/11448624/).
52. Maddox-Hyttel P, Alexopoulos NI, Vajta G, Lewis I, Rogers P, Cann L, et al. Immunohistochemical and ultrastructural characterization of the initial post-hatching development of bovine embryos. *Reproduction*. 2003; 125(4):607–23. PMID: [12683931](https://pubmed.ncbi.nlm.nih.gov/12683931/).
53. Nowotschin S, Hadjantonakis AK. Cellular dynamics in the early mouse embryo: from axis formation to gastrulation. *Current opinion in genetics & development*. 2010; 20(4):420–7. doi: [10.1016/j.gde.2010.05.008](https://doi.org/10.1016/j.gde.2010.05.008) PMID: [20566281](https://pubmed.ncbi.nlm.nih.gov/20566281/); PubMed Central PMCID: [PMC2908213](https://pubmed.ncbi.nlm.nih.gov/PMC2908213/).
54. Skreb N, Solter D, Damjanov I. Developmental biology of the murine egg cylinder. *The International journal of developmental biology*. 1991; 35(3):161–76. PMID: [1814399](https://pubmed.ncbi.nlm.nih.gov/1814399/).
55. Stephenson RO, Rossant J, Tam PP. Intercellular interactions, position, and polarity in establishing blastocyst cell lineages and embryonic axes. *Cold Spring Harbor perspectives in biology*. 2012; 4(11). doi: [10.1101/cshperspect.a008235](https://doi.org/10.1101/cshperspect.a008235) PMID: [23125013](https://pubmed.ncbi.nlm.nih.gov/23125013/); PubMed Central PMCID: [PMC3536338](https://pubmed.ncbi.nlm.nih.gov/PMC3536338/).

56. Vejlsted M, Avery B, Schmidt M, Greve T, Alexopoulos N, Maddox-Hyttel P. Ultrastructural and immunohistochemical characterization of the bovine epiblast. *Biology of reproduction*. 2005; 72(3):678–86. doi: [10.1095/biolreprod.104.034348](https://doi.org/10.1095/biolreprod.104.034348) PMID: [15537864](https://pubmed.ncbi.nlm.nih.gov/15537864/).
57. Vejlsted M, Du Y, Vajta G, Maddox-Hyttel P. Post-hatching development of the porcine and bovine embryo—defining criteria for expected development in vivo and in vitro. *Theriogenology*. 2006; 65(1):153–65. doi: [10.1016/j.theriogenology.2005.09.021](https://doi.org/10.1016/j.theriogenology.2005.09.021) PMID: [16257443](https://pubmed.ncbi.nlm.nih.gov/16257443/).
58. Jedrusik A, Parfitt DE, Guo G, Skamagki M, Grabarek JB, Johnson MH, et al. Role of Cdx2 and cell polarity in cell allocation and specification of trophectoderm and inner cell mass in the mouse embryo. *Genes & development*. 2008; 22(19):2692–706. doi: [10.1101/gad.486108](https://doi.org/10.1101/gad.486108) PMID: [18832072](https://pubmed.ncbi.nlm.nih.gov/18832072/); PubMed Central PMCID: [PMC2559904](https://pubmed.ncbi.nlm.nih.gov/PMC2559904/).
59. Strumpf D, Mao CA, Yamanaka Y, Ralston A, Chawengsaksophak K, Beck F, et al. Cdx2 is required for correct cell fate specification and differentiation of trophectoderm in the mouse blastocyst. *Development*. 2005; 132(9):2093–102. doi: [10.1242/dev.01801](https://doi.org/10.1242/dev.01801) PMID: [15788452](https://pubmed.ncbi.nlm.nih.gov/15788452/).
60. Artus J, Chazaud C. A close look at the mammalian blastocyst: epiblast and primitive endoderm formation. *Cellular and molecular life sciences: CMLS*. 2014; 71(17):3327–38. doi: [10.1007/s00018-014-1630-3](https://doi.org/10.1007/s00018-014-1630-3) PMID: [24794628](https://pubmed.ncbi.nlm.nih.gov/24794628/).
61. Kuijk EW, van Tol LT, Van de Velde H, Wubbolts R, Welling M, Geijsen N, et al. The roles of FGF and MAP kinase signaling in the segregation of the epiblast and hypoblast cell lineages in bovine and human embryos. *Development*. 2012; 139(5):871–82. doi: [10.1242/dev.071688](https://doi.org/10.1242/dev.071688) PMID: [22278923](https://pubmed.ncbi.nlm.nih.gov/22278923/); PubMed Central PMCID: [PMC3274353](https://pubmed.ncbi.nlm.nih.gov/PMC3274353/).
62. Kuijk EW, Du Puy L, Van Tol HT, Oei CH, Haagsman HP, Colenbrander B, et al. Differences in early lineage segregation between mammals. *Developmental dynamics: an official publication of the American Association of Anatomists*. 2008; 237(4):918–27. doi: [10.1002/dvdy.21480](https://doi.org/10.1002/dvdy.21480) PMID: [18330925](https://pubmed.ncbi.nlm.nih.gov/18330925/).
63. Pfister S, Steiner KA, Tam PP. Gene expression pattern and progression of embryogenesis in the immediate post-implantation period of mouse development. *Gene expression patterns: GEP*. 2007; 7(5):558–73. doi: [10.1016/j.modgep.2007.01.005](https://doi.org/10.1016/j.modgep.2007.01.005) PMID: [17331809](https://pubmed.ncbi.nlm.nih.gov/17331809/).
64. Chazaud C, Yamanaka Y, Pawson T, Rossant J. Early lineage segregation between epiblast and primitive endoderm in mouse blastocysts through the Grb2-MAPK pathway. *Developmental cell*. 2006; 10(5):615–24. doi: [10.1016/j.devcel.2006.02.020](https://doi.org/10.1016/j.devcel.2006.02.020) PMID: [16678776](https://pubmed.ncbi.nlm.nih.gov/16678776/).
65. El-Hashash AH, Warburton D, Kimber SJ. Genes and signals regulating murine trophoblast cell development. *Mechanisms of development*. 2010; 127(1–2):1–20. doi: [10.1016/j.mod.2009.09.004](https://doi.org/10.1016/j.mod.2009.09.004) PMID: [19755154](https://pubmed.ncbi.nlm.nih.gov/19755154/); PubMed Central PMCID: [PMC2865247](https://pubmed.ncbi.nlm.nih.gov/PMC2865247/).
66. Cai KQ, Capo-Chichi CD, Rula ME, Yang DH, Xu XX. Dynamic GATA6 expression in primitive endoderm formation and maturation in early mouse embryogenesis. *Developmental dynamics: an official publication of the American Association of Anatomists*. 2008; 237(10):2820–9. doi: [10.1002/dvdy.21703](https://doi.org/10.1002/dvdy.21703) PMID: [18816845](https://pubmed.ncbi.nlm.nih.gov/18816845/); PubMed Central PMCID: [PMC2739724](https://pubmed.ncbi.nlm.nih.gov/PMC2739724/).
67. Saga Y, Miyagawa-Tomita S, Takagi A, Kitajima S, Miyazaki J, Inoue T. MesP1 is expressed in the heart precursor cells and required for the formation of a single heart tube. *Development*. 1999; 126(15):3437–47. PMID: [10393122](https://pubmed.ncbi.nlm.nih.gov/10393122/).
68. Solter D, Damjanov I, Skreb N. Ultrastructure of mouse egg-cylinder. *Zeitschrift fur Anatomie und Entwicklungsgeschichte*. 1970; 132(4):291–8. PMID: [5492120](https://pubmed.ncbi.nlm.nih.gov/5492120/).
69. Enders AC, Given RL, Schlafke S. Differentiation and migration of endoderm in the rat and mouse at implantation. *The Anatomical record*. 1978; 190(1):65–77. doi: [10.1002/ar.1091900107](https://doi.org/10.1002/ar.1091900107) PMID: [626417](https://pubmed.ncbi.nlm.nih.gov/626417/).
70. Bielinska M, Narita N, Wilson DB. Distinct roles for visceral endoderm during embryonic mouse development. *The International journal of developmental biology*. 1999; 43(3):183–205. PMID: [10410899](https://pubmed.ncbi.nlm.nih.gov/10410899/).
71. Bernard O, Ripoché MA, Bennett D. Distribution of maternal immunoglobulins in the mouse uterus and embryo in the days after implantation. *The Journal of experimental medicine*. 1977; 145(1):58–75. PMID: [830790](https://pubmed.ncbi.nlm.nih.gov/830790/); PubMed Central PMCID: [PMC2180582](https://pubmed.ncbi.nlm.nih.gov/PMC2180582/).
72. Rachman F, Casimiri V, Bernard O. Maternal immunoglobulins G, A and M in mouse uterus and embryo during the postimplantation period. *Journal of reproductive immunology*. 1984; 6(1):39–47. PMID: [6363695](https://pubmed.ncbi.nlm.nih.gov/6363695/).
73. Takasuga S, Horie Y, Sasaki J, Sun-Wada GH, Kawamura N, Iizuka R, et al. Critical roles of type III phosphatidylinositol phosphate kinase in murine embryonic visceral endoderm and adult intestine. *Proceedings of the National Academy of Sciences of the United States of America*. 2013; 110(5):1726–31. doi: [10.1073/pnas.1213212110](https://doi.org/10.1073/pnas.1213212110) PMID: [23322734](https://pubmed.ncbi.nlm.nih.gov/23322734/); PubMed Central PMCID: [PMC3562790](https://pubmed.ncbi.nlm.nih.gov/PMC3562790/).

74. Wallingford MC, Giachelli CM. Loss of Pit-1 results in abnormal endocytosis in the yolk sac visceral endoderm. *Mechanisms of development*. 2014; 133:189–202. doi: [10.1016/j.mod.2014.08.001](https://doi.org/10.1016/j.mod.2014.08.001) PMID: [25138534](https://pubmed.ncbi.nlm.nih.gov/25138534/); PubMed Central PMCID: PMC4207432.
75. Inman KE, Downs KM. Localization of Brachyury (T) in embryonic and extraembryonic tissues during mouse gastrulation. *Gene expression patterns: GEP*. 2006; 6(8):783–93. doi: [10.1016/j.modgep.2006.01.010](https://doi.org/10.1016/j.modgep.2006.01.010) PMID: [16545989](https://pubmed.ncbi.nlm.nih.gov/16545989/).
76. Hogan BL, Tilly R. Cell interactions and endoderm differentiation in cultured mouse embryos. *Journal of embryology and experimental morphology*. 1981; 62:379–94. PMID: [7276820](https://pubmed.ncbi.nlm.nih.gov/7276820/).
77. Degrelle SA, Champion E, Cabau C, Piumi F, Reinaud P, Richard C, et al. Molecular evidence for a critical period in mural trophoblast development in bovine blastocysts. *Developmental biology*. 2005; 288(2):448–60. doi: [10.1016/j.ydbio.2005.09.043](https://doi.org/10.1016/j.ydbio.2005.09.043) PMID: [16289134](https://pubmed.ncbi.nlm.nih.gov/16289134/).
78. Chiba N, Comaills V, Shiotani B, Takahashi F, Shimada T, Tajima K, et al. Homeobox B9 induces epithelial-to-mesenchymal transition-associated radioresistance by accelerating DNA damage responses. *Proceedings of the National Academy of Sciences of the United States of America*. 2012; 109(8):2760–5. doi: [10.1073/pnas.1018867108](https://doi.org/10.1073/pnas.1018867108) PMID: [21930940](https://pubmed.ncbi.nlm.nih.gov/21930940/); PubMed Central PMCID: PMC3286905.
79. Topisirovic I, Kentsis A, Perez JM, Guzman ML, Jordan CT, Borden KL. Eukaryotic translation initiation factor 4E activity is modulated by HOXA9 at multiple levels. *Mol Cell Biol*. 2005; 25(3):1100–12. PMID: [15657436](https://pubmed.ncbi.nlm.nih.gov/15657436/). doi: [10.1128/MCB.25.3.1100-1112.2005](https://doi.org/10.1128/MCB.25.3.1100-1112.2005)
80. Bridoux L, Bergiers I, Draime A, Halbout M, Deneyer N, Twizere JC, et al. KPC2 relocalizes HOXA2 to the cytoplasm and decreases its transcriptional activity. *Biochimica et biophysica acta*. 2015; 1849(10):1298–311. doi: [10.1016/j.bbagr.2015.08.006](https://doi.org/10.1016/j.bbagr.2015.08.006) PMID: [26303204](https://pubmed.ncbi.nlm.nih.gov/26303204/).
81. Jedrusik A, Bruce AW, Tan MH, Leong DE, Skamagki M, Yao M, et al. Maternally and zygotically provided Cdx2 have novel and critical roles for early development of the mouse embryo. *Developmental biology*. 2010; 344(1):66–78. doi: [10.1016/j.ydbio.2010.04.017](https://doi.org/10.1016/j.ydbio.2010.04.017) PMID: [20430022](https://pubmed.ncbi.nlm.nih.gov/20430022/); PubMed Central PMCID: PMC2954319.
82. Li L, Zheng P, Dean J. Maternal control of early mouse development. *Development*. 2010; 137(6):859–70. doi: [10.1242/dev.039487](https://doi.org/10.1242/dev.039487) PMID: [20179092](https://pubmed.ncbi.nlm.nih.gov/20179092/); PubMed Central PMCID: PMC2834456.
83. Keramari M, Razavi J, Ingman KA, Patsch C, Edenhofer F, Ward CM, et al. Sox2 is essential for formation of trophectoderm in the preimplantation embryo. *PloS one*. 2010; 5(11):e13952. doi: [10.1371/journal.pone.0013952](https://doi.org/10.1371/journal.pone.0013952) PMID: [21103067](https://pubmed.ncbi.nlm.nih.gov/21103067/); PubMed Central PMCID: PMC2980489.
84. Coticchio G, Dal Canto M, Mignini Renzini M, Guglielmo MC, Brambillasca F, Turchi D, et al. Oocyte maturation: gamete-somatic cells interactions, meiotic resumption, cytoskeletal dynamics and cytoplasmic reorganization. *Human reproduction update*. 2015; 21(4):427–54. doi: [10.1093/humupd/dmv011](https://doi.org/10.1093/humupd/dmv011) PMID: [25744083](https://pubmed.ncbi.nlm.nih.gov/25744083/).
85. Hayashida T, Takahashi F, Chiba N, Brachtel E, Takahashi M, Godin-Heymann N, et al. HOXB9, a gene overexpressed in breast cancer, promotes tumorigenicity and lung metastasis. *Proceedings of the National Academy of Sciences of the United States of America*. 2010; 107(3):1100–5. doi: [10.1073/pnas.0912710107](https://doi.org/10.1073/pnas.0912710107) PMID: [20080567](https://pubmed.ncbi.nlm.nih.gov/20080567/); PubMed Central PMCID: PMC2824265.
86. Sha L, Dong L, Lv L, Bai L, Ji X. HOXB9 promotes epithelial-to-mesenchymal transition via transforming growth factor-beta1 pathway in hepatocellular carcinoma cells. *Clinical and experimental medicine*. 2015; 15(1):55–64. doi: [10.1007/s10238-014-0276-7](https://doi.org/10.1007/s10238-014-0276-7) PMID: [25081022](https://pubmed.ncbi.nlm.nih.gov/25081022/).
87. Zhan J, Niu M, Wang P, Zhu X, Li S, Song J, et al. Elevated HOXB9 expression promotes differentiation and predicts a favourable outcome in colon adenocarcinoma patients. *British journal of cancer*. 2014; 111(5):883–93. doi: [10.1038/bjc.2014.387](https://doi.org/10.1038/bjc.2014.387) PMID: [25025961](https://pubmed.ncbi.nlm.nih.gov/25025961/); PubMed Central PMCID: PMC4150282.
88. Myers M, Pangas SA. Regulatory roles of transforming growth factor beta family members in folliculogenesis. *Wiley interdisciplinary reviews Systems biology and medicine*. 2010; 2(1):117–25. doi: [10.1002/wsbm.21](https://doi.org/10.1002/wsbm.21) PMID: [20836015](https://pubmed.ncbi.nlm.nih.gov/20836015/).
89. Ozawa M, Sakatani M, Yao J, Shanker S, Yu F, Yamashita R, et al. Global gene expression of the inner cell mass and trophectoderm of the bovine blastocyst. *BMC developmental biology*. 2012; 12:33. doi: [10.1186/1471-213X-12-33](https://doi.org/10.1186/1471-213X-12-33) PMID: [23126590](https://pubmed.ncbi.nlm.nih.gov/23126590/); PubMed Central PMCID: PMC3514149.
90. Hosseini SM, Dufort I, Caballero J, Moulavi F, Ghanaei HR, Sirard MA. Transcriptome profiling of bovine inner cell mass and trophectoderm derived from in vivo generated blastocysts. *BMC developmental biology*. 2015; 15:49. doi: [10.1186/s12861-015-0096-3](https://doi.org/10.1186/s12861-015-0096-3) PMID: [26681441](https://pubmed.ncbi.nlm.nih.gov/26681441/); PubMed Central PMCID: PMC4683974.
91. Tsark EC, Adamson ED, Withers GE 3rd, Wiley LM. Expression and function of amphiregulin during murine preimplantation development. *Molecular reproduction and development*. 1997; 47(3):271–83. doi: [10.1002/\(SICI\)1098-2795\(199707\)47:3<271::AID-MRD6>3.0.CO;2-I](https://doi.org/10.1002/(SICI)1098-2795(199707)47:3<271::AID-MRD6>3.0.CO;2-I) PMID: [9170107](https://pubmed.ncbi.nlm.nih.gov/9170107/).

92. Lee JH, Lee E, Biswas D, Jeung CS, Lee GS, Hyun SH, et al. Amphiregulin promotes the proliferation of trophoblast cells during preimplantation development of porcine embryos. *Theriogenology*. 2009; 72(8):1023–31. doi: [10.1016/j.theriogenology.2009.05.021](https://doi.org/10.1016/j.theriogenology.2009.05.021) PMID: [19729194](https://pubmed.ncbi.nlm.nih.gov/19729194/).
93. Slager HG, Lawson KA, van den Eijnden-van Raaij AJ, de Laat SW, Mummery CL. Differential localization of TGF-beta 2 in mouse preimplantation and early postimplantation development. *Developmental biology*. 1991; 145(2):205–18. PMID: [2040369](https://pubmed.ncbi.nlm.nih.gov/2040369/).
94. Paria BC, Jones KL, Flanders KC, Dey SK. Localization and binding of transforming growth factor-beta isoforms in mouse preimplantation embryos and in delayed and activated blastocysts. *Developmental biology*. 1992; 151(1):91–104. PMID: [1577201](https://pubmed.ncbi.nlm.nih.gov/1577201/).
95. Gupta A, Bazer FW, Jaeger LA. Differential expression of beta transforming growth factors (TGF beta 1, TGF beta 2, and TGF beta 3) and their receptors (type I and type II) in peri-implantation porcine conceptuses. *Biology of reproduction*. 1996; 55(4):796–802. PMID: [8879492](https://pubmed.ncbi.nlm.nih.gov/8879492/).
96. Ravelich SR, Shelling AN, Wells DN, Peterson AJ, Lee RS, Ramachandran A, et al. Expression of TGF-beta1, TGF-beta2, TGF-beta3 and the receptors TGF-betaRI and TGF-betaRII in placentomes of artificially inseminated and nuclear transfer derived bovine pregnancies. *Placenta*. 2006; 27(2–3):307–16. doi: [10.1016/j.placenta.2005.03.002](https://doi.org/10.1016/j.placenta.2005.03.002) PMID: [15955560](https://pubmed.ncbi.nlm.nih.gov/15955560/).
97. Munson L, Wilhite A, Boltz VF, Wilkinson JE. Transforming growth factor beta in bovine placentas. *Biology of reproduction*. 1996; 55(4):748–55. PMID: [8879485](https://pubmed.ncbi.nlm.nih.gov/8879485/).
98. Barcroft LC, Hay-Schmidt A, Caveney A, Gilfoyle E, Overstrom EW, Hyttel P, et al. Trophectoderm differentiation in the bovine embryo: characterization of a polarized epithelium. *Journal of reproduction and fertility*. 1998; 114(2):327–39. PMID: [10070362](https://pubmed.ncbi.nlm.nih.gov/10070362/).
99. Goyal JJ, Van Cauwenberge A, Alexandre H. Respective roles of protein tyrosine kinases and protein kinases C in the upregulation of beta-catenin distribution, and compaction in mouse preimplantation embryos: a pharmacological approach. *Biol Cell*. 2000; 92(7):513–26. PMID: [11229602](https://pubmed.ncbi.nlm.nih.gov/11229602/).
100. Ohsugi M, Hwang SY, Butz S, Knowles BB, Solter D, Kemler R. Expression and cell membrane localization of catenins during mouse preimplantation development. *Developmental dynamics: an official publication of the American Association of Anatomists*. 1996; 206(4):391–402. doi: [10.1002/\(SICI\)1097-0177\(199608\)206:4<391::AID-AJA5>3.0.CO;2-D](https://doi.org/10.1002/(SICI)1097-0177(199608)206:4<391::AID-AJA5>3.0.CO;2-D) PMID: [8853988](https://pubmed.ncbi.nlm.nih.gov/8853988/).
101. De Vries WN, Evsikov AV, Haac BE, Fancher KS, Holbrook AE, Kemler R, et al. Maternal beta-catenin and E-cadherin in mouse development. *Development*. 2004; 131(18):4435–45. doi: [10.1242/dev.01316](https://doi.org/10.1242/dev.01316) PMID: [15306566](https://pubmed.ncbi.nlm.nih.gov/15306566/).
102. Larue L, Ohsugi M, Hirchenhain J, Kemler R. E-cadherin null mutant embryos fail to form a trophectoderm epithelium. *Proceedings of the National Academy of Sciences of the United States of America*. 1994; 91(17):8263–7. PMID: [8058792](https://pubmed.ncbi.nlm.nih.gov/8058792/); PubMed Central PMCID: [PMC44586](https://pubmed.ncbi.nlm.nih.gov/PMC44586/).
103. Ohsugi M, Larue L, Schwarz H, Kemler R. Cell-junctional and cytoskeletal organization in mouse blastocysts lacking E-cadherin. *Developmental biology*. 1997; 185(2):261–71. doi: [10.1006/dbio.1997.8560](https://doi.org/10.1006/dbio.1997.8560) PMID: [9187087](https://pubmed.ncbi.nlm.nih.gov/9187087/).
104. Kan NG, Stemmler MP, Junghans D, Kanzler B, de Vries WN, Dominis M, et al. Gene replacement reveals a specific role for E-cadherin in the formation of a functional trophectoderm. *Development*. 2007; 134(1):31–41. doi: [10.1242/dev.02722](https://doi.org/10.1242/dev.02722) PMID: [17138661](https://pubmed.ncbi.nlm.nih.gov/17138661/).
105. Stephenson RO, Yamanaka Y, Rossant J. Disorganized epithelial polarity and excess trophectoderm cell fate in preimplantation embryos lacking E-cadherin. *Development*. 2010; 137(20):3383–91. doi: [10.1242/dev.050195](https://doi.org/10.1242/dev.050195) PMID: [20826529](https://pubmed.ncbi.nlm.nih.gov/20826529/).
106. Kimber SJ, Bentley J, Ciemerych M, Moller CJ, Bock E. Expression of N-CAM in fertilized pre- and periimplantation and parthenogenetically activated mouse embryos. *Eur J Cell Biol*. 1994; 63(1):102–13. PMID: [8005097](https://pubmed.ncbi.nlm.nih.gov/8005097/).
107. Berg DK, Smith CS, Pearton DJ, Wells DN, Broadhurst R, Donnison M, et al. Trophectoderm lineage determination in cattle. *Developmental cell*. 2011; 20(2):244–55. doi: [10.1016/j.devcel.2011.01.003](https://doi.org/10.1016/j.devcel.2011.01.003) PMID: [21316591](https://pubmed.ncbi.nlm.nih.gov/21316591/).
108. van den Akker E, Forlani S, Chawengsaksophak K, de Graaff W, Beck F, Meyer BI, et al. Cdx1 and Cdx2 have overlapping functions in anteroposterior patterning and posterior axis elongation. *Development*. 2002; 129(9):2181–93. PMID: [11959827](https://pubmed.ncbi.nlm.nih.gov/11959827/).
109. Rawat VP, Thoene S, Naidu VM, Arseni N, Heilmeier B, Metzeler K, et al. Overexpression of CDX2 perturbs HOX gene expression in murine progenitors depending on its N-terminal domain and is closely correlated with deregulated HOX gene expression in human acute myeloid leukemia. *Blood*. 2008; 111(1):309–19. doi: [10.1182/blood-2007-04-085407](https://doi.org/10.1182/blood-2007-04-085407) PMID: [17855634](https://pubmed.ncbi.nlm.nih.gov/17855634/).
110. Amesse LS, Moulton R, Zhang YM, Pfaff-Amesse T. Expression of HOX gene products in normal and abnormal trophoblastic tissue. *Gynecologic oncology*. 2003; 90(3):512–8. PMID: [13678718](https://pubmed.ncbi.nlm.nih.gov/13678718/).

111. Murasawa H, Takashima R, Yamanouchi K, Tojo H, Tachi C. Comparative analysis of HOXC-9 gene expression in murine hemochorial and caprine synepitheliochorial placentae by in situ hybridization. *The Anatomical record*. 2000; 259(4):383–94. PMID: [10903530](#).
112. Takashima RM H, Yamanouchi K, Tojo H, Tachi C. Survey of Homeobox Genes Expressed in Hemochorial Placentae of Mice (*Mus musculus*) and in Epitheliochorial/Syndesmochorial Placentae of Shiba Goats (*Capra hircus* var. Shiba) *Journal of reproduction and development*. 1999; 45:363–74.
113. Zhang YM, Xu B, Rote N, Peterson L, Amesse LS. Expression of homeobox gene transcripts in trophoblastic cells. *American journal of obstetrics and gynecology*. 2002; 187(1):24–32. PMID: [12114884](#).
114. Hu D, Cross JC. Development and function of trophoblast giant cells in the rodent placenta. *The International journal of developmental biology*. 2010; 54(2–3):341–54. doi: [10.1387/ijdb.082768dh](#) PMID: [19876834](#).
115. Peter AT. Bovine placenta: a review on morphology, components, and defects from terminology and clinical perspectives. *Theriogenology*. 2013; 80(7):693–705. doi: [10.1016/j.theriogenology.2013.06.004](#) PMID: [23849255](#).
116. Mitchell MD, Peiris HN, Kobayashi M, Koh YQ, Duncombe G, Illanes SE, et al. Placental exosomes in normal and complicated pregnancy. *American journal of obstetrics and gynecology*. 2015; 213(4 Suppl):S173–81. doi: [10.1016/j.ajog.2015.07.001](#) PMID: [26428497](#).
117. Choi DS, Park JO, Jang SC, Yoon YJ, Jung JW, Choi DY, et al. Proteomic analysis of microvesicles derived from human colorectal cancer ascites. *Proteomics*. 2011; 11(13):2745–51. doi: [10.1002/pmic.201100022](#) PMID: [21630462](#).
118. Hong BS, Cho JH, Kim H, Choi EJ, Rho S, Kim J, et al. Colorectal cancer cell-derived microvesicles are enriched in cell cycle-related mRNAs that promote proliferation of endothelial cells. *BMC genomics*. 2009; 10:556. doi: [10.1186/1471-2164-10-556](#) PMID: [19930720](#); PubMed Central PMCID: PMC2788585.
119. Wada Y. Vacuoles in mammals: a subcellular structure indispensable for early embryogenesis. *Bioarchitecture*. 2013; 3(1):13–9. doi: [10.4161/bioa.24126](#) PMID: [23572040](#); PubMed Central PMCID: PMC3639239.
120. Kawamura N, Sun-Wada GH, Aoyama M, Harada A, Takasuga S, Sasaki T, et al. Delivery of endosomes to lysosomes via microautophagy in the visceral endoderm of mouse embryos. *Nature communications*. 2012; 3:1071. doi: [10.1038/ncomms2069](#) PMID: [22990867](#).
121. Maurer ME, Cooper JA. Endocytosis of megalin by visceral endoderm cells requires the Dab2 adaptor protein. *Journal of cell science*. 2005; 118(Pt 22):5345–55. doi: [10.1242/jcs.02650](#) PMID: [16263760](#).
122. Yang DH, Smith ER, Roland IH, Sheng Z, He J, Martin WD, et al. Disabled-2 is essential for endodermal cell positioning and structure formation during mouse embryogenesis. *Developmental biology*. 2002; 251(1):27–44. PMID: [12413896](#).
123. Scotti M, Kmita M. Recruitment of 5' Hoxa genes in the allantois is essential for proper extra-embryonic function in placental mammals. *Development*. 2012; 139(4):731–9. doi: [10.1242/dev.075408](#) PMID: [22219351](#); PubMed Central PMCID: PMC4508127.
124. Chawengsaksophak K, de Graaff W, Rossant J, Deschamps J, Beck F. Cdx2 is essential for axial elongation in mouse development. *Proceedings of the National Academy of Sciences of the United States of America*. 2004; 101(20):7641–5. doi: [10.1073/pnas.0401654101](#) PMID: [15136723](#); PubMed Central PMCID: PMC419659.